Targeted knockout of a chemokine-like gene increases anxiety and fear responses

Jung-Hwa Choi[a,1], Yun-Mi Jeong[a,1], Sujin Kim[b,c], Boyoung Lee[c], Krishan Ariyasiri[a], Hyun-Taek Kim[a], Seung-Hyun Jung[a], Kyu-Seok Hwang[a], Tae-Ik Choi[a], Chul O Park[d], Won-Ki Huh[d], Matthias Carl[e], Jill A. Rosenfeld[f], Salmo Raskin[g], Alan Ma[h,i], Jozef Gecz[j,k], Hyung-Goo Kim[l,m], Jin-Soo Kim[n,o], Ho-Chul Shin[p], Doo-Sang Park[p], Robert Gerlai[q], Bradley B. Jamieson[r,s], Joon S. Kim[r,s], Karl J. Iremonger[r,s], Sang H. Lee[t], Hee-Sup Shin[b,c,2], and Cheol-Hee Kim[a,2]

[a]Department of Biology, Chungnam National University, 34134 Daejeon, South Korea; [b]Institute for Basic Science School, University of Science and Technology, 34113 Daejeon, South Korea; [c]Center for Cognition and Sociality, Institute for Basic Science, 34141 Daejeon, South Korea; [d]Department of Biological Sciences, Seoul National University, 151-747 Seoul, South Korea; [e]Laboratory of Translational Neurogenetics, Center for Integrative Biology, University of Trento, 38123 Trento, Italy; [f]Department of Molecular & Human Genetics, Baylor College of Medicine, Houston, TX 77030; [g]Group for Advanced Molecular Investigation, Health and Biosciences School, Pontifícia Universidade Católica do Paraná, 80215-901 Curitiba Paraná, Brazil; [h]Department of Genetics, Nepean Hospital Sydney, University of Sydney, NSW 2006, Australia; [i]Discipline of Child & Adolescent Health, Children's Hospital at Westmead Clinical School, University of Sydney, NSW 2006, Australia; [j]School of Medicine and The Robinson Research Institute, University of Adelaide, Adelaide 5000, Australia; [k]Healthy Mothers and Babies, South Australian Health and Medical Research Institute, Adelaide 5000, Australia; [l]Department of OB/GYN, Augusta University, Augusta, GA 30912; [m]Department of Neuroscience and Regenerative Medicine, Augusta University, Augusta, GA 30912; [n]Center for Genome Engineering, Institute for Basic Science, Seoul National University, 151-747 Seoul, South Korea; [o]Department of Chemistry, Seoul National University, 151-747 Seoul, South Korea; [p]Korea Research Institute of Bioscience and Biotechnology, 305-806 Daejeon, South Korea; [q]Department of Psychology, University of Toronto Mississauga, Mississauga, ON L5L 1C6, Canada; [r]Department of Physiology, University of Otago, 9054 Dunedin, New Zealand; [s]Centre for Neuroendocrinology, University of Otago, 9054 Dunedin, New Zealand; and [t]Department of Pharmacology & Toxicology, Neuroscience Research Institute, Medical College of Wisconsin, WI 53226

Edited by Alex Schier, Harvard University, Cambridge, MA, and accepted by Editorial Board Member Kathryn V. Anderson December 21, 2017 (received for review May 30, 2017)

Emotional responses, such as fear and anxiety, are fundamentally important behavioral phenomena with strong fitness components in most animal species. Anxiety-related disorders continue to represent a major unmet medical need in our society, mostly because we still do not fully understand the mechanisms of these diseases. Animal models may speed up discovery of these mechanisms. The zebrafish is a highly promising model organism in this field. Here, we report the identification of a chemokine-like gene family, *samdori* (*sam*), and present functional characterization of one of its members, *sam2*. We show exclusive mRNA expression of *sam2* in the CNS, predominantly in the dorsal habenula, telencephalon, and hypothalamus. We found knockout (KO) zebrafish to exhibit altered anxiety-related responses in the tank, scototaxis and shoaling assays, and increased *crh* mRNA expression in their hypothalamus compared with wild-type fish. To investigate generalizability of our findings to mammals, we developed a *Sam2* KO mouse and compared it to wild-type littermates. Consistent with zebrafish findings, homozygous KO mice exhibited signs of elevated anxiety. We also found bath application of purified SAM2 protein to increase inhibitory postsynaptic transmission onto CRH neurons of the paraventricular nucleus. Finally, we identified a human homolog of *SAM2*, and were able to refine a candidate gene region encompassing *SAM2*, among 21 annotated genes, which is associated with intellectual disability and autism spectrum disorder in the 12q14.1 deletion syndrome. Taken together, these results suggest a crucial and evolutionarily conserved role of *sam2* in regulating mechanisms associated with anxiety.

chemokine-like | anxiety | fear | knockout | zebrafish

Emotional responses, such as fear (responses to the appearance of well-defined and clearly present aversive stimuli) and anxiety (responses seen under aversive contexts in which the clear presence of fear inducing stimuli cannot be ascertained or these stimuli are continuously present and diffuse), are essential behavioral phenomena that have strong fitness components in all species (1). Anxiety-related disorders continue to represent a major unmet medical need in our society. Despite concerted efforts to develop anxiolytic and antidepressant pharmacotherapies, a large proportion of patients remain unresponsive to medication (2). This is due to the fact that we still do not fully understand the mechanisms of these diseases. To facilitate mechanistic analysis and to speed up the process of target identification and psychopharmacological characterization of compounds, animal models have been proposed.

Emotional responses, such as fear and anxiety, are regulated by various neuromodulators (3). Recently, studies have raised the possibility that chemokines may also possess neuromodulatory functions. Chemokines are small, secreted signaling proteins that commonly act as chemo-attractants to guide the migration of cells of the immune system. Importantly, chemokines are also expressed in neurons and glial cells of the central nervous system (CNS); while their role in the brain has mainly been associated with

Significance

Emotion-related responses, such as fear and anxiety, are important behavioral phenomena in most animal species, as well as in humans. However, the underlying mechanisms of fear and anxiety in animals and in humans are still largely unknown, and anxiety disorders continue to represent a large unmet medical need in the human clinic. Animal models may speed up discovery of these mechanisms and may also lead to betterment of human health. Herein, we report the identification of a chemokine-like gene family, *samdori* (*sam*), and present functional characterization of *sam2*. We observed increased anxiety-related responses in both zebrafish and mouse knockout models. Taken together, these results support a crucial and evolutionarily conserved role of *sam2* in regulating anxiety-like behavior.

Author contributions: J.-H.C. and C.-H.K. designed research; J.-H.C., Y.-M.J., S.K., B.L., H.-T.K., S.-H.J., K.-S.H., T.-I.C., C.O.P., W.-K.H., M.C., H.-C.S., D.-S.P., B.B.J., and J.S.K. performed research; J.A.R., S.R., A.M., J.G., and H.-G.K. contributed to human genetic data; J.-H.C., K.A., J.-S.K., B.B.J., J.S.K., K.J.I., S.H.L., H.-S.S., and C.-H.K. analyzed data; and J.-H.C., R.G., S.H.L., and C.-H.K. wrote the paper.

The authors declare no conflict of interest.

This article is a PNAS Direct Submission. A.S. is a guest editor invited by the Editorial Board.

[1]J.-H.C. and Y.-M.J. contributed equally to this work.

[2]To whom correspondence may be addressed. Email: shin@ibs.re.kr or zebrakim@cnu.ac.kr.

This article contains supporting information online at www.pnas.org/lookup/suppl/doi:10.1073/pnas.1707663115/-/DCSupplemental.

neuro-inflammatory responses, it is becoming more evident that chemokines in the brain may hold other functions (4–6).

Emotion dysregulation can lead to serious behavioral problems and impaired social interaction associated with a variety of disease conditions, including attention deficit hyperactivity disorder, bipolar disorder, and posttraumatic stress disorder (7, 8). Despite the paucity of proper treatment options for such disorders, the exploration of possible underlying genetic and biological mechanisms has been slow. The identification of novel genes associated with emotional behavior and understanding neural mechanisms of higher brain function remains a major goal of biology.

The use of animal models has greatly aided this research. The zebrafish (*Danio rerio*) has emerged as a promising model organism for the study of complex neuropsychiatric diseases because of the well-defined behavioral phenotypes of this species (9), and because of its evolutionarily conserved brain structures and functions. One example of such a brain structure is the habenula (Hb), which is connected with the subpallium and hypothalamus, and is implicated in fear, anxiety, addiction, and mood disorders (10, 11).

The zebrafish is useful for large-scale forward genetic screens to discover novel genes involved in CNS development, an approach we have utilized (12, 13). Over 10 y ago we discovered a chemokine-like gene family, called *samdori* (*sam*), using genetic screens (i.e., insertional mutagenesis with a unique dual reporter system) (*SI Appendix*, Fig. S1). We present herein the body of work that has extended from initial gene discovery and encompasses various analyses of the physiological functions of this family.

A member of this family, s*am2* exhibits exclusive brain-specific expression, predominantly in neurons of the dorsal Hb (dHb), as well as the telencephalic area and hypothalamus. Here, we report the development of a zebrafish null mutant (KO) in which this gene is silenced. We investigate the effect of this null mutation using behavioral assays developed to induce and measure fear and anxiety responses. To investigate the generalizability of our findings obtained with zebrafish, we also report herein the development and analysis of a mouse null mutant in which the mammalian homolog of the zebrafish *sam2* gene is silenced. We found phenotypical alterations in the *Sam2* KO mice that are consistent with those we observed in the zebrafish null mutants, suggesting that *Sam2* is critical for regulating anxiety across such evolutionarily distant species as mammals and fish.

In addition, we also analyzed a variety of markers in the zebrafish *sam2* KO (colocalization studies), which uncovered changes in mRNA expression of the gene encoding corticotropin-releasing hormone (CRH), a hormone involved in stress and anxiety responses in mammals (14). We followed up this investigation with whole-cell patch-clamp electrophysiological recordings from CRH neurons in the mouse hypothalamus, and found that Sam2 modulated GABAergic synaptic transmission on CRH neurons.

Finally, we investigated whether mutations in the human genome potentially affecting *SAM2* function may have functional, behavioral consequences. We identified patients with microdeletions/microduplications in 12q14.1, including *SAM2*, who suffered from a variety of behavioral and intellectual problems. Using six copy-number variations (CNVs), we were able to refine the candidate gene region encompassing *SAM2* among 21 annotated genes at 12q14.1.

In summary, we describe the discovery of a chemokine-like protein family and provide initial functional characterization of one of its members, s*am2*. Taken together, our multidisciplinary results demonstrate a potentially crucial role of this candidate gene in the regulation of emotion-related behaviors across evolutionarily distant species, and delineate a target that may allow the development of effective pharmacotherapy for human CNS disorders associated with altered fear, anxiety, and stress.

Results

Identification of *samdori2*. Using insertional mutagenesis to identify novel functional genes, we isolated a chemokine-like gene, *sam* [also called *TAFA* (15) and *FAM19A* in the National Center for Biotechnology Information database] (*SI Appendix*, Fig. S1). Subsequently, we also isolated other members of *sam* family based upon the sequences in the database. We have identified eight members in the zebrafish *sam* gene family, and found them highly conserved in mouse and human at the amino acid sequence level (*SI Appendix*, Fig. S2 *A–E*). All Sam proteins exhibited 10 regularly spaced cysteine residues with a pattern of $CX_7CCX_{13}CXCX_{14}CX_{11}CX_4CX_5CX_{10}C$, a sequence similar to that of CC-type chemokines (15).

Using whole-mount in situ hybridization in zebrafish, we found all *sam* genes to be exclusively expressed in the CNS at larval stages (*SI Appendix*, Fig. S2 *F–O*). Among them, we focused on the functional analysis of the *sam2* gene, because we found *sam2* to be predominantly expressed in the dHb of adult fish (Fig. 1). To further characterize *sam2*-expressing cells, we performed whole-mount in situ hybridization in larval and adult fish brains using various neuronal markers. In addition to dHb, *sam2*-expressing cells were also detected in the telencephalon and otic neurons in larvae (*SI Appendix*, Fig. S3*A*). In situ hybridization of adult brain and serial sectioning revealed the detailed expressions of *sam2* in the medial zone of the dorsal telencephalic area (Dm), the dorsal nucleus of the ventral telencephalon (Vd), preoptic area of hypothalamus (PPa), and other hypothalamic regions (ATN, anterior tuberal nucleus; Hc, caudal zone of periventricular hypothalamus; Hd, dorsal zone of periventricular hypothalamus; and PTN, posterior tuberal nucleus) (Fig. 1 and *SI Appendix*, Fig. S3 and Table S1). To assess the distribution of *sam2* within excitatory and inhibitory circuits, we performed double in situ hybridization with GABAergic markers (16, 17) and glutamatergic markers (16, 17). We found *sam2*$^+$ cells in *GAD67*/*gad1b*-expressing cells in the Vd, central nucleus of the ventral region (Vc), and PPa (Fig. 1*D* and *SI Appendix*, Fig. S4). In the diencephalon, *sam2*-expressing cells were observed adjacent to *GAD65*/*gad2*$^+$ cells in the hypothalamic area, such as the ATN and PTN, and periventricular hypothalamus (*SI Appendix*, Fig. S4). With the glutamatergic markers, *sam2* mRNA was partially overlapped with *vglut2b* in the Dm but not in other forebrain regions (Fig. 1 *B* and *C*). In addition, *sam2* was found to overlap with *vglut2a* in the dorsal region of the Hb (Fig. 1*F*). Expression of *sam2* in the Hb was further examined by costaining with dHb-specific *kctd12.1* (*lov*) (18, 19) or ventral Hb (vHb)-specific marker, *aoc1* or dHb/vHb marker *fam84b* (20) (*SI Appendix*, Fig. S5 *A–E*). *sam2* expression was found not to colocalize with known markers of dopaminergic (21), oxytocinergic (22), or hypocretinergic (23) neurons (Fig. 1 and *SI Appendix*, Fig. S5 *F–H′*). The Hb has been implicated in the regulation of emotion, including anxiety, fear, depression, and reward (7, 24). The fish telencephalic regions are homologous to the mammalian amygdala (Dm) and striatum (Vd), structures that are known to play fundamental roles in emotion-related behaviors in mammals (25). Thus, expression of the *sam2* gene detected in the dHb, telencephalic areas (Dm, Vd), and hypothalamic regions prompted us to investigate its function in the regulation of emotion.

Normal Development of Neuronal Cells in *sam2* KO Fish. To investigate the function of *sam2*, we created two *sam2* KO zebrafish lines, taking advantage of targeted mutagenesis utilizing zinc-finger nucleases (ZFNs) (26, 27). The 5-bp deletion (*sam2*^{cnu1}) and 17-bp deletion (*sam2*^{cnu2}) of the two alleles induced

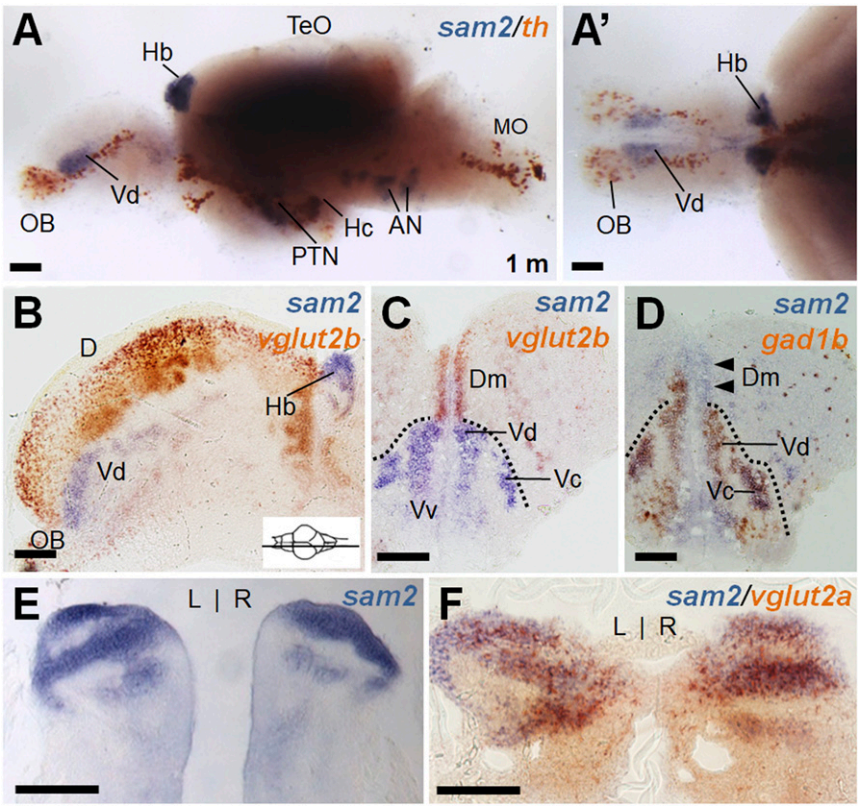

Fig. 1. Characterization of *sam2*-expressing cells in the adult zebrafish brain. (*A* and *A′*) Whole-mount two color in situ hybridization of a dissected zebrafish brain with *sam2* and a dopaminergic neuron marker, *th*. Anterior is to the left; lateral (*A*) and dorsal view (*A′*). The *sam2* expression region did not overlap with th^+ neurons. Prominent *sam2* expression is seen in the Vd and Hb as well as hypothalamic regions. (*B–D*) Section images of brain hybridized with *sam2/vglut2b* (*B*, sagittal section; *C*, cross-section) or *sam2/gad1b* (*D*). (*E* and *F*) Cross-section of Hb region stained with *sam2* alone (*E*) or *sam2/vglut2a* (*F*) probes. AN, auditory nerve; D, area dorsalis telencephlali; Dc, central zone of area dorsalis telencephali; MO, medulla oblongata; OB, olfactory bulb; TeO, optic tectum; Vv, ventral nucleus of area ventral telencephali. (Scale bars, 100 μm.)

frame-shift mutations (Fig. 2 *A–B′*), which lead to alteration of the protein-coding sequence (*SI Appendix*, Fig. S6*A*). Both *sam2* KO lines showed normal morphology during embryonic development (Fig. 2 *C* and *C′*), survived to adulthood, and were fertile. To test whether *sam2* is necessary for the development of specific neuronal cell-types, we examined the expression of various molecular markers in *sam2* KO zebrafish (*SI Appendix*, Fig. S6 *B–G′*). Compared with wild-type fish, we could not detect any significant differences in the expression patterns of dopaminergic neuronal markers [tyrosine hydroxylase (*th*) (21), dopamine transporter (*dat*) (28), and nuclear receptor related 1 protein (*nurr-1*) (28)], serotonergic neuronal markers [tryptophan hydroxylase raphe (*tphR*) and 5-hydroxytryptophan (5-HT)] (29), oxytocinergic neuronal marker oxytocin (*oxt*) (22), and interpeduncular nucleus (IPN) marker somatostatin1.1 (*sst1.1*) (30). Moreover, *sam2* KO embryos showed normal expression of neurohormonal genes (*SI Appendix*, Fig. S6 *H–M′*), including hypocretin/orexin (*hcrt*) (23), melanin concentrating hormone (*mch*) (31), agouti related protein homolog (*agrp*) (32), neuropeptide Y (*npy*) (33), and pet-1 (*fev*; ETS oncogene family) (29). In addition, we observed normal hypothalamus–locus coeruleus projections in progenies of the *Tg(hcrt:mEGFP)* (23) transgenic line crossed to the $sam2^{cnu1}$ mutant (*SI Appendix*, Fig. S6 *N–O′*). Moreover, the targeting of Hb efferent axons innervating the IPN appeared to be largely unaffected in the *Et(-1.0otpa:mmGFP)hd1* (34) transgenic embryos crossed to $sam2^{cnu1}$ KO fish (Fig. 2 *D* and *E′*). Therefore, we conclude that *sam2* is not directly involved in the generation, migration, and axonal growth of neurons.

Increase of Anxiety-Like Responses in *sam2* Mutant Fish. We next examined whether the loss of *sam2* affects behaviors associated with anxiety using the open (novel) tank (35, 36) and dark/light preference (scototaxis) (37) tests. Anxiety and fear are related phenomena, but can be distinguished. Responses induced by a present and clearly detectable aversive stimulus are regarded as fear responses (behavior aimed at the avoidance of the stimulus), whereas anxiety-like behavior is found under diffuse aversive conditions: that is, without the appearance or clear presence of such stimuli. Novelty is an aversive context without the presence of specific fear-inducing stimuli, and thus novel test situations are often used to quantify anxiety. In the novel tank, when placed individually, $sam2^{cnu1}$ KO fish showed normal locomotor activity, as indicated by no changes in total distance traveled (Fig. 3*A*) ($sam2^{+/+}$, 4,359.29 ± 218.68 cm, $n = 18$; $sam2^{-/-}$, 4,088.71 ± 249.83 cm, $n = 28$) and in average velocity (Fig. 3*B*) ($sam2^{+/+}$, 7.63 ± 0.37 cm/s, $n = 18$; $sam2^{-/-}$, 7.02 ± 0.41 cm/s, $n = 28$), compared with control sibling fish. Moreover, there were no significant differences in the frequency of transition to the upper half of the test tank between $sam2^{cnu1}$ KO and control fish (Fig. 3*C*) ($sam2^{+/+}$, 30 ± 6.93, $n = 18$; $sam2^{-/-}$, 34.86 ± 4.19, $n = 28$), a measure of vertical exploration. However, $sam2^{cnu1}$ KO fish exhibited behavioral characteristics indicative of elevated levels of anxiety, including an increased number of erratic movements (1, 38) (Fig. 3*D*) ($sam2^{+/+}$, 52.67 ± 9.19, $n = 18$; $sam2^{-/-}$, 142.14 ± 12.50, $n = 28$) and number of freezing events (35, 36) (Fig. 3*E*) ($sam2^{+/+}$, 0.17 ± 0.09, $n = 18$; $sam2^{-/-}$, 0.44 ± 0.10, $n = 27$). Freezing is a typical response seen in aversive contexts and can be used to quantify the level of anxiety in a variety of species,

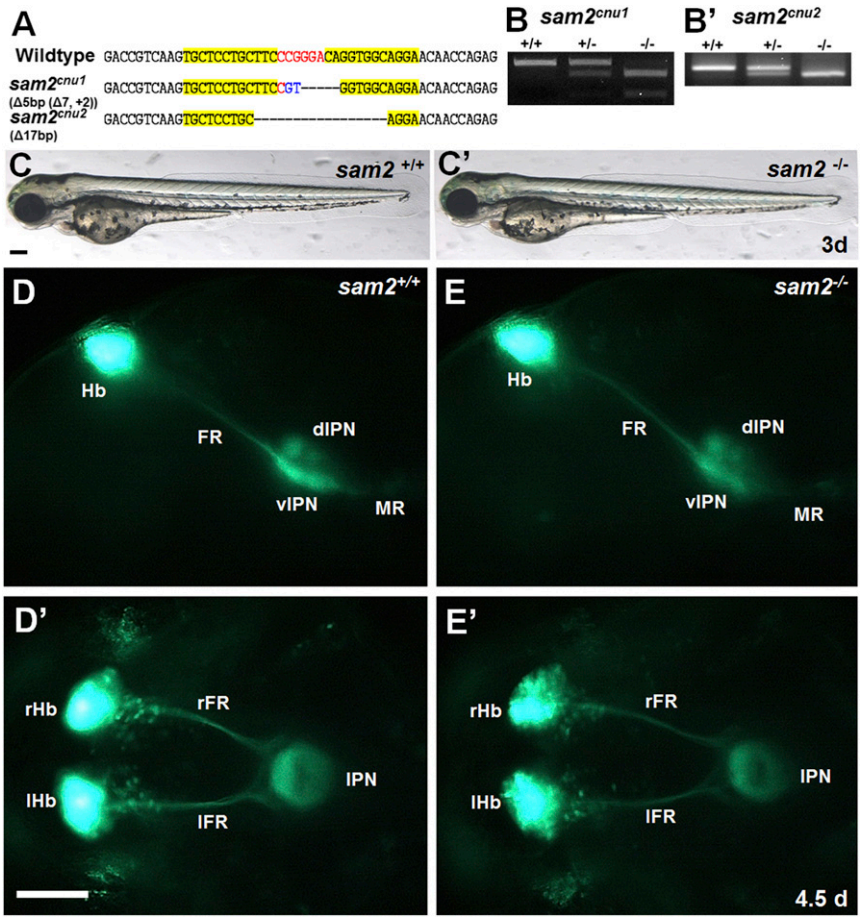

Fig. 2. Generation of *sam2* KO fish using ZFNs. (*A*) DNA sequencing analysis of two *sam2* KO alleles (*sam2*^{cnu1} and *sam2*^{cnu2}) with 5-bp and 17-bp deletion, respectively. Yellow mark, *Left* and *Right* ZFN-binding regions; red, spacer. (*B* and *B*′) Allele-specific genotyping of *sam2*^{cnu1} and *sam2*^{cnu2} KO fish by genomic PCR and digestion for *Btg*I site (CCGTGG) newly created in *sam2*^{cnu1}. (*C* and *C*′) Normal morphology of *sam2*^{cnu1} KO embryo at 3 d. (*D*–*E*′) Projections of Hb efferent axons targeting the lPN in the *Et(-1.0otpa:mmGFP)hd1* transgenic *sam2*^{cnu1} KO fish were not visibly affected. Lateral views (*D* and *E*) and dorsal views (*D*′ and *E*′). dlPN, dorsal lPN; FR, fasciculus retroflexus; lFR, *Left* FR; lHb, *Left* Hb; MR, median raphe; rFR, *Right* FR; rHb, *Right* HbvlPN, ventral lPN. (Scale bar, 100 μm.)

including zebrafish and rodents (36). Erratic movement has also been shown to be a characteristic sign of anxiety or fear in zebrafish (36, 39). Thus, our results indicate that *sam2* may be involved in the regulation of anxiety-like responses in zebrafish. To further investigate anxiety-like behavior in *sam2*^{cnu1} KO fish, we also measured thigmotaxis (avoidance of open areas) in the novel tank. Increased thigmotaxis in novel contexts has been interpreted as a sign of anxiety (36). *sam2*^{cnu1} KO fish showed higher preference for the corner over the center of the test tank (*SI Appendix*, Fig. S7*A*) (*sam2*$^{+/+}$ at the corner, 21.22 ± 0.56 s, at the center 34.15 ± 0.70 s, $n = 12$; *sam2*$^{-/-}$ at the corner, 26.83 ± 0.95 s, at the center, 29.14 ± 0.89 s, $n = 12$). The light/dark paradigm is another frequently employed test of fear and anxiety in zebrafish and rodents (37), and zebrafish have been shown to exhibit scototaxis (i.e., dark preference). Consistent with the results obtained in the novel tank task, in the light/dark paradigm, adult *sam2*^{cnu1} KO fish traveled a shorter distance (Fig. 3*F*) (*sam2*$^{+/+}$, 1,533.59 ± 191.18 cm, $n = 18$; *sam2*$^{-/-}$, 788.88 ± 116.09 cm, $n = 24$), spent less time in the white arena (*SI Appendix*, Fig. S7 *B* and *C*) (*sam2*$^{+/+}$ in the black, 733.125 ± 80.66 s, in the white 168.38 ± 80.42 s, $n = 18$; *sam2*$^{-/-}$ in the black, 811.5 ± 64.81 s, in the white 104.08 ± 87.67 s, $n = 24$), and exhibited reduced frequency of black/white transitions compared with wild-type (Fig. 3*G*) (*sam2*$^{+/+}$, 81.67 ± 8.74, $n = 18$; *sam2*$^{-/-}$, 38.69 ± 4.36, $n = 24$), alterations that further corroborate the notion that the null mutant fish suffered from elevated levels of anxiety. These results suggest that *sam2* may regulate emotion-related behaviors.

Increase of Social Cohesion in *sam2* KO Fish. Zebrafish form groups, a behavior called shoaling. One of the adaptive functions of this social behavior has been shown to be predator-avoidance. Measures of shoal cohesion have been successfully utilized in the analysis and modeling of anxiety and fear in vertebrates, including zebrafish (1, 36). To test whether *sam2* KO fish exhibit altered shoaling behavior, a group of five *sam2* KO fish were placed in a novel tank at a time and monitored by 3D video tracking. We recorded the swim paths of the fish in the group for 30 min (Fig. 4 and *SI Appendix*, S8 *A*–*B*′) (40). Because wild-type zebrafish typically take 10 min to habituate to a novel tank (41), we analyzed the behavior of fish at two time points: early phase (before habituation, 5–8 min) and late phase (after habituation, 13–16 min) of the session. During the early phase, both *sam2* KO and control fish showed typical anxiety-like responses by staying close to the bottom of the tank. However, at the late phase control sibling fish started to swim in the middle and the top layers of the water (Fig. 4 *A* and *B*), a response interpreted as reduction of anxiety. In sharp contrast, *sam2* KO fish remained near the bottom of the tank (Fig. 4 *A*′ and *B*′ and Movie S1), suggesting impaired habituation to the novel environment (i.e.,

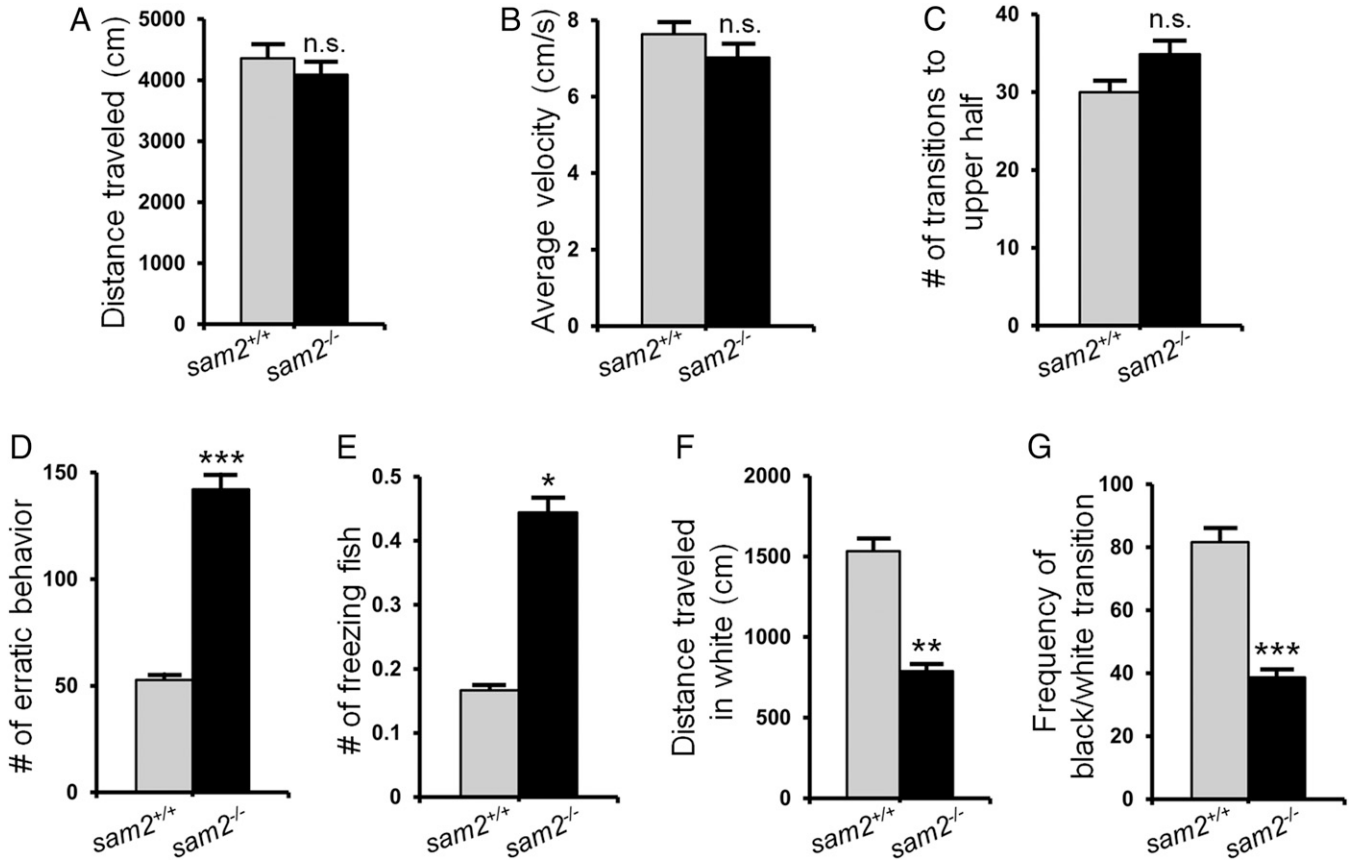

Fig. 3. Increase of anxiety-related behaviors in *sam2*^{cnu1} KO zebrafish. (*A–E*) Novel tank tests of individually placed fish. The distance traveled (*A*) (*sam2*$^{+/+}$, $n = 18$; *sam2*$^{-/-}$, $n = 28$; Cohen's $d = 0.24$; Mann–Whitney $U = 181$, $P = 0.11$), average velocity (*B*) (*sam2*$^{+/+}$, $n = 18$; *sam2*$^{-/-}$, $n = 28$; Cohen's $d = 0.32$; Mann–Whitney $U = 171$, $P = 0.07$), and transition to upper half (*C*) (*sam2*$^{+/+}$, $n = 18$; *sam2*$^{-/-}$, $n = 28$; Cohen's $d = 0.19$; Mann–Whitney $U = 202$, $P = 0.27$) were not significantly changed in *sam2* KO fish. However, the frequency of erratic behavior (*D*) (*sam2*$^{+/+}$, $n = 18$; *sam2*$^{-/-}$, $n = 28$; Cohen's $d = 1.65$; Mann–Whitney $U = 41$, $P < 0.00001$) and the number of freezing fish (*E*) (*sam2*$^{+/+}$, $n = 18$; *sam2*$^{-/-}$, $n = 27$; Cohen's $d = 0.62$; $P = 0.042$, Student's *t* test) were increased in *sam2* KO fish. (*F* and *G*) Black/white preference (scototaxis) test. Distance traveled in white arena (*F*) (*sam2*$^{+/+}$, $n = 18$; *sam2*$^{-/-}$, $n = 24$; Cohen's $d = 1.06$; Mann–Whitney $U = 85$, $P = 0.0032$) and frequency of transitions (*G*) (*sam2*$^{+/+}$, $n = 18$; *sam2*$^{-/-}$, $n = 24$; Cohen's $d = 1.42$; Mann–Whitney $U = 61.5$, $P = 0.00016$) were measured. $*P < 0.05$; $**P < 0.01$; $***P < 0.001$; ns, not significant ($P > 0.05$).

maintenance of elevated levels of anxiety) in *sam2* KO fish. We next examined social cohesion in *sam2* KO zebrafish by measuring the distance between a focal fish and each of its shoal members (interindividual distance) (41–43). Control fish significantly increased their mean interindividual distance from the early phase to the late phase, suggesting the reduction of novelty-induced anxiety (Fig. 4 *C* and *C′*). However, *sam2* KO fish did not show such changes in mean individual distance, and maintained the same strong shoal cohesion (Fig. 4*C′* and *SI Appendix*, Fig. S8). The effect size (Cohen's *d*) for cohesion of the control and *sam2*^{cnu1} KO fish was $d = -0.063$ at the early phase (5–8 min) and $d = -0.80$ at the late phase (13–16 min). These results confirm that *sam2* KO mutants exhibit elevated levels of anxiety compared with wild-type fish.

Excessive Anxiety/Fear Behavior in *sam2* KO Fish in Response to Alarm Substance. The above behavioral paradigms are considered to induce anxiety-like responses, because they do not use specific clearly present aversive stimuli. To test fear responses, we conducted another test in which an aversive stimulus was specifically provided and was clearly present during the test. A clearly present aversive stimulus that may be delivered in a well-defined manner to the zebrafish is the alarm substance (38). Among other behavioral responses, the alarm substance has been shown to induce a reliable alteration in shoaling that may be used to measure fear in zebrafish (38). In our study, we examined changes in shoal cohesion in response to administration of the alarm substance (*SI Appendix*, Fig. S9). Both control and *sam2* KO fish exhibited increased shoal cohesion (reduced distance among shoal members) in response to the delivery of alarm substance. However, the relative decrease of interindividual distance in *sam2* KO fish was more robust compared with that of wild-type control siblings. The effect size between before and after alarm treatment was $d = -1.09$ for control and $d = -1.22$ for *sam2*^{cnu1} KO fish, respectively. The effect size between control and *sam2*^{cnu1} KO fish was $d = -0.96$ before and $d = -1.57$ after alarm treatment. This was despite that the former had already displayed small interindividual distance even before the delivery of the alarm substance (*SI Appendix*, Fig. S9*E*). Thus, taken together these results demonstrate elevated anxiety and fear in *sam2* KO fish.

Increase of mRNA Expression of Stress-Related *crhb* in *sam2* KO Fish. Aversive stimuli that induce fear and anxiety are expected to lead to physiological changes: for example, neurohormonal stress responses mediated by the hypothalamic–pituitary–adrenal (HPA) axis (14, 44). A previous study demonstrated that disruption of glucocorticoid-negative feedback of the HPA axis resulted in elevated cortisol levels and anxiety-like behavior in zebrafish (14). We hypothesized that the increased level of anxiety in *sam2* KO

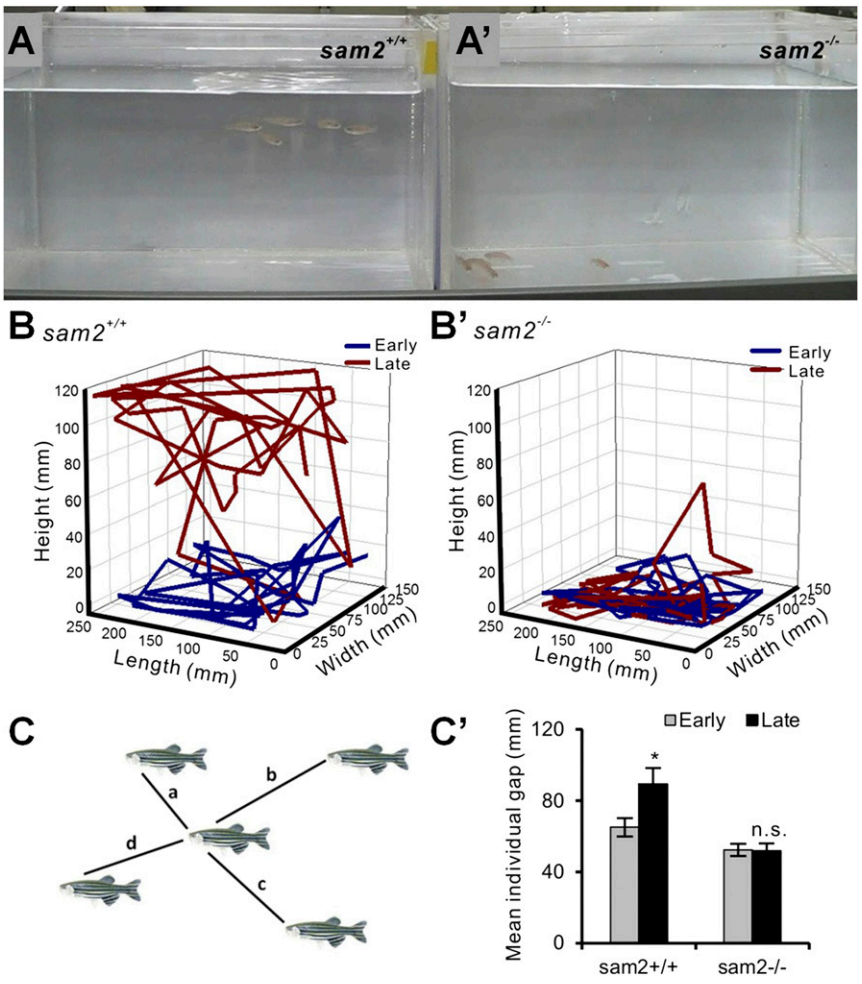

Fig. 4. Anxiety-like behavior and increased social cohesion in *sam2*^{cnu1} KO fish. Five fish (3-mo-old male siblings) were placed as a group in a novel tank. (*A* and *A*′) A snapshot of video tracking after 20-min novel tank test. (*B* and *B*′) Temporal 3D reconstructions of video tracking before habituation (early, 5–8 min, blue; Cohen's $d = -0.063$) and after habituation (late, 13–16 min, red; Cohen's $d = -0.80$) to the novel environment. (*C* and *C*′) Measurement of social cohesion as the mean individual gap. We measured the distance between the focal fish and one of its shoal members (lines a, b, c, and d; interindividual distances). $P = 0.02$ for control and $P = 0.88$ for *sam2* KO fish (*sam2*$^{+/+}$, $n = 5$; *sam2*$^{-/-}$, $n = 5$). *$P < 0.05$; ns, not significant ($P > 0.05$).

fish may also be associated with dysregulation of the HPA axis. Using in situ hybridization, we found *sam2*^{cnu1} KO fish to exhibit elevated *crhb* expression, an important HPA axis marker, in the PPa compared with wild-type (see, for example, Fig. 6 *A*–*D*). Increased *crhb* mRNA levels in the PPa, a region homologous to the mammalian paraventricular nucleus (PVN), is consistent with previous reports of dysregulated HPA axis function in zebrafish and mice (14, 45).

***Sam2* KO Mice also Exhibit Anxiety-Like and Fear-Related Behaviors.** To investigate whether the role of *sam2* in anxiety and fear is evolutionarily conserved or specific only to the zebrafish, we generated a *Sam2* KO mouse line (*SI Appendix*, Fig. S10) and compared the behavior of these mutants to wild-type littermates. *Sam2* showed brain-specific expression in mouse similar to that of zebrafish, having a higher expression level in the hippocampus and Hb but not in the PVN (*SI Appendix*, Fig. S11). We found *Sam2* KO mice to spend significantly less time in the open arms on an elevated plus maze (Fig. 5*C*) (*Sam2*$^{+/+}$ mice, $38.3 \pm 9.16\%$, $n = 11$; *Sam2*$^{-/-}$ mice, $19.66 \pm 6.66\%$, $n = 8$) and to show increased freezing in both the contextual (Fig. 5*E*) (*Sam2*$^{+/+}$ mice, $42.86 \pm 8.08\%$, $n = 11$; *Sam2*$^{-/-}$ mice, $69.74 \pm 6.12\%$, $n = 7$) and cued fear-conditioning tests (Fig. 5*F*) (*Sam2*$^{+/+}$ mice, $40.33 \pm 6.32\%$, $n = 11$; *Sam2*$^{-/-}$ mice, $70.95 \pm 4.97\%$, $n = 7$) compared with wild-type littermates. The elevated freezing in the null mutant mice was not due to a motor function-related change, as both mutant and wild-type animals exhibited similar levels of freezing on training day (Fig. 5*D*) [two-way repeated-measures ANOVA, Time × Group interaction: $F(3, 48) = 0.48$, $P = 0.69$, *Sam2*$^{+/+}$ mice, $n = 11$; *Sam2*$^{-/-}$ mice, $n = 7$]. Body weight (Fig. 5*A*) (*Sam2*$^{+/+}$ mice, 24.86 ± 0.59 g, $n = 25$; *Sam2*$^{-/-}$ mice, 24.07 ± 0.39 g, $n = 10$) and total locomotion on an open-field test (Fig. 5*B*) [two-way repeated-measures ANOVA, Time × Group interaction: $F(5, 75) = 0.32$, $P = 0.89$, *Sam2*$^{+/+}$ mice, $n = 11$; *Sam2*$^{-/-}$ mice, $n = 6$] were not significantly different between *Sam2* KO and wild-type control mice. Collectively, the *Sam2* KO mice exhibited phenotypical alterations reminiscent of the KO zebrafish, suggesting that *Sam2* plays a potentially critical and evolutionally conserved role in regulating anxiety- and fear-related behavioral responses.

Increase in the Frequency of Spontaneous Inhibitory Postsynaptic Currents by SAM2. Increased activity in the stress axis is one of the most enduring findings in both animal models and human patients with anxiety. Elevated fear and anxiety responses in mice are accompanied by both *Crh* mRNA overexpression and increased excitability of the PVN neurons (14, 45). Similarly, selective knockout of *Crh* in the PVN results in reduced anxiety (46). Therefore, we hypothesized that *Sam2* could regulate CRH neuron excitability in the PVN. To investigate this hypothesis, we exposed PVN CRH neurons to a 5-min-long bath application of SAM2 (1 μM) (*SI Appendix*, Fig. S12). In response to this treatment, we found a significant increase in the frequency of spontaneous inhibitory postsynaptic currents (sIPSC); that is, $162.5 \pm 39.76\%$ of baseline ($n = 11$, $P < 0.01$, Wilcoxon signed-rank matched-pairs test) (Fig. 6 *F* and *G*). We found no significant change in the sIPSC amplitude, however ($100.9 \pm 5.3\%$ of baseline, $n = 11$, $P = 0.15$, Wilcoxon signed-rank matched-pairs

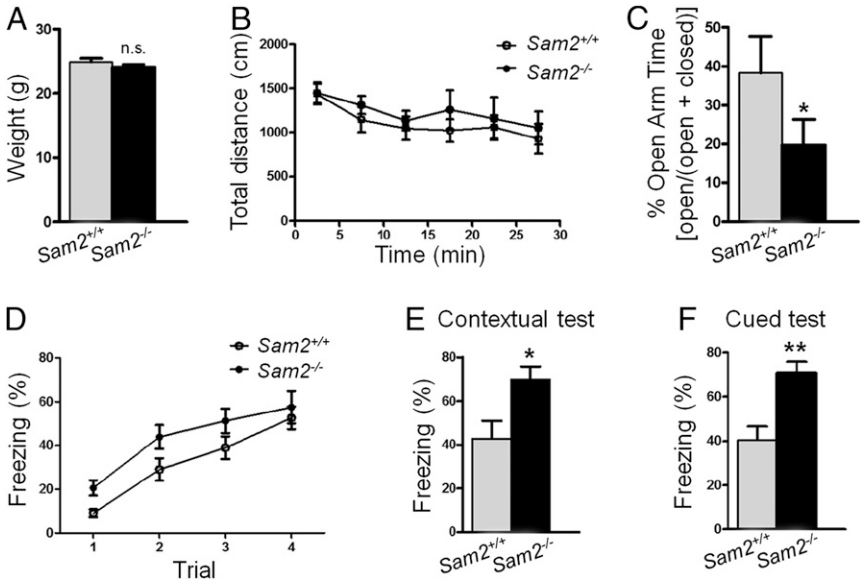

Fig. 5. Increase of anxiety-related behaviors in *Sam2* KO mice. (*A*) *Sam2* KO mice have normal body weight ($Sam2^{+/+}$, $n = 25$; $Sam2^{-/-}$, $n = 10$; Cohen's $d = 0.31$; unpaired two-tailed, Mann–Whitney $U = 124$, $P = 0.98$). (*B*) *Sam2* KO mice show normal total locomotion in an open-field test [$Sam2^{+/+}$, $n = 11$; $Sam2^{-/-}$, $n = 6$; two-way repeated-measures ANOVA, Time × Group interaction: $F(5, 75) = 0.32$, $P = 0.89$]. (*C*) *Sam2* KO mice spent significantly less time in the open arms on an elevated plus maze ($Sam2^{+/+}$, $n = 11$; $Sam2^{-/-}$, $n = 8$; Cohen's $d = 0.74$; unpaired one-tailed, Mann–Whitney $U = 23$, $P = 0.045$). (*D*) *Sam2* KO mice show similar levels of freezing response during training days [$Sam2^{+/+}$, $n = 11$; $Sam2^{-/-}$, $n = 7$; two-way repeated-measures ANOVA, Time × Group interaction: $F(3, 48) = 0.48$, $P = 0.69$]. (*E*) *Sam2* KO mice show higher freezing behavior in contextual test 24 h after training ($Sam2^{+/+}$, $n = 11$; $Sam2^{-/-}$, $n = 7$; Cohen's $d = 1.21$; unpaired two-tailed, Mann–Whitney $U = 15$, $P = 0.035$). (*F*) *Sam2* KO mice show higher freezing behavior in cued test 24 h after training ($Sam2^{+/+}$, $n = 11$; $Sam2^{-/-}$, $n = 7$; Cohen's $d = 1.75$; unpaired two-tailed, Mann–Whitney $U = 7$, $P = 0.0028$). *$P < 0.05$; **$P < 0.01$; ns, not significant ($P > 0.05$).

test) (Fig. 6*H*). We also observed no significant differences in evoked IPSC (eIPSC) amplitude and paired-pulse ratio (Fig. 6 *I*–J, and *K*). Thus, we conclude that SAM2 is able to significantly increase the frequency, but not the amplitude, of spontaneous GABAergic currents onto CRH neurons, rather than the amplitude of evoked GABAergic currents. These observations indicate that SAM2 may control tonic GABAergic inputs onto CRH neurons.

Comparative Genomic Mapping Using Six CNVs at 12q14.1. Mutations (i.e., microdeletions or duplications) arising at the 12q14.1 region are characterized by a previously unreported feature set including craniofacial anomalies, cryptorchidism, intellectual disability, autism, and behavioral problems. Using six informative CNVs, we were able to refine the candidate gene region encompassing *SAM2* at 12q14.1 (Fig. 7). We found deletions in two females, GC42855 and GC48823, sized 6.2 Mb (chr12: 62,097,144 to 68,266,543/hg19) and 5.1 Mb (chr12: 58,011,515 to 63,115,073/hg19), respectively (Fig. 7). GC48823 is 4-y-old with autism and seizures, whereas GC42855 is 6-y-old with developmental delay. A 1-Mb minimal overlapping region of these two deletions at 12q14.1 contains four genes including *SAM2*. Furthermore, we identified two more small CNVs in the DECIPHER (database of chromosomal imbalance and phenotype in humans using Ensembl resources) human genome variants database (47) overlapping the gene. Among them, patient 288660 with an 887-kb duplication (chr12: 61,271,591 to 62,158,216/hg19) has attention deficit hyperactivity disorder, autism spectrum disorder, and generalized joint laxity. However, this duplication overlaps only the 3′ end of the gene and may not disrupt its function. More importantly, patient 290951 has inherited an 880-kb deletion (chr12: 62,038,772 to 62,918,916/hg19) encompassing *SAM2* and *USP15* in a three-generation pedigree from the maternal grandfather through his mother with significant intellectual disability. Patient 290951 had a clinical diagnosis of autism spectrum disorder, behavioral difficulties, and severe speech and language delay. Overall he performed in the mild range of intellectual disability, as did his mother and maternal grandfather, who all had the same deletion. His unaffected brother, sister, and uncle did not inherit the deletion (Fig. 7 *B*–*D*). In mice, *Usp15* is ubiquitously expressed in various tissues. *Usp15* KO mice had normal survival rate and did not show abnormalities in development, although its deficiency enhanced T cell response against bacterial infection and tumor (48). A 61-kb minimal overlapping region of these four CNVs flanked by two blue vertical dotted lines encompasses the 56-kb 3′ end of *SAM2*. These data suggest that *SAM2* contributes to the neurological phenotype of these patients. DECIPHER also has two additional small CNVs in this region, not including *SAM2*: child 251128 with behavioral problems, low-set ears, intellectual disability, and speech delay, has inherited an 886-kb deletion (chr12: 62,799,199 to 63,684,842/hg19) from a parent with similar phenotypes, and patient 287965 with a 224-kb duplication (chr12: 61,544,595 to 61,768,510/hg19) has global developmental delay.

Discussion

The functions of chemokines are well documented in the immune system. However, the potential role of CNS-expressed chemokines and chemokine-like proteins as neuromodulators is still largely unknown. In this study, we identified a chemokine-like *sam* gene family, showing CNS-specific expression. We provide empirical evidence for the involvement of a chemokine-like protein, SAM2, in vertebrate brain function and behavior associated with the regulation of anxiety and fear responses.

The targeted knockout of a single gene, *sam2*, in zebrafish produced an anxiogenic phenotype reminiscent of changes induced by Hb ablation. For example, ablation of the dHb in zebrafish has been shown to increase freezing and other behavioral signs of anxiety (25, 49–51). The anxiety-like and fear-related behavioral changes we detected in our zebrafish null mutants were also observed in our mouse KO model, highlighting the evolutionarily conserved role of *Sam2* in the regulation of anxiety and fear in vertebrates.

Our in situ hybridization results showed the presence of *sam2* transcripts in the telencephalic areas (Dm, Vd) and hypothalamic regions of the zebrafish brain. The Dm and Vd are known as the homologous regions for the mammalian amygdala and striatum, respectively. The involvement of these regions in anxiety has been demonstrated by numerous behavioral and molecular studies using both mammalian species and zebrafish (25, 52). In addition to traditional measures of anxiety and fear—such as freezing, thigmotaxis, or erratic movement—we also found evidence of increased anxiety in our zebrafish null mutants by measuring their shoaling responses. Shoaling is an adaptive and natural antipredatory behavior utilized in the analysis and modeling of vertebrate anxiety and fear (1). Furthermore, *sam2* KO fish, when exposed to the alarm substance, exhibited significantly increased shoaling (reduction of interindividual

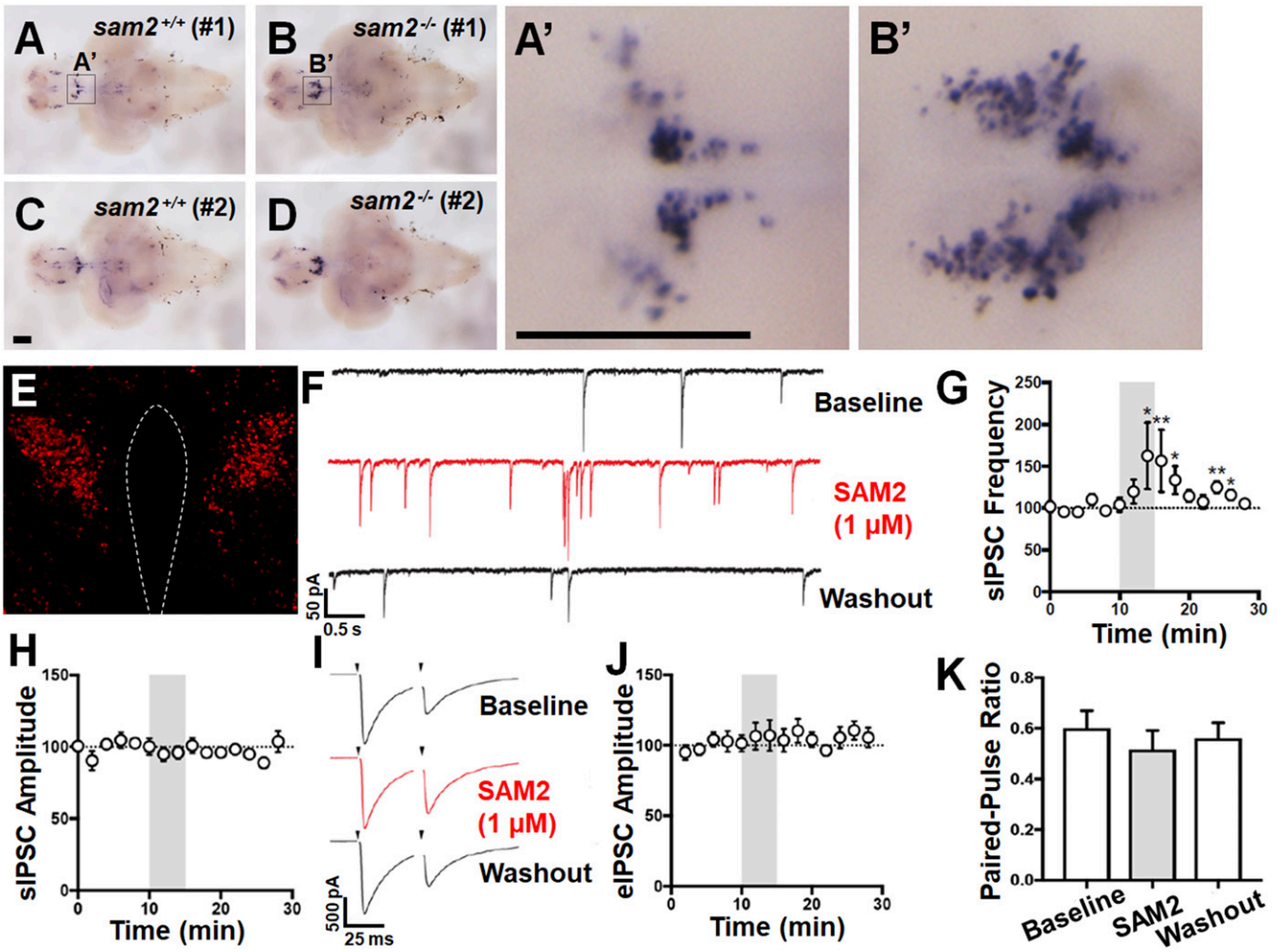

Fig. 6. Increase of mRNA expression of stress-related *crhb* in *sam2*^{cnu1} KO fish and spontaneous inhibitory postsynaptic currents onto CRH neurons by SAM2. (*A–D*) Increase of *crhb* mRNA expression in *sam2*^{cnu1} KO fish (*sam2*$^{+/+}$, $n = 6$; *sam2*$^{-/-}$, $n = 6$). Ventral views of the whole brain of control *sam2*$^{+/+}$ (*A* and *C*) and *sam2*$^{-/-}$ KO fish (*B* and *D*). (*A′* and *B′*) Higher magnifications of the boxed regions in *A* and *B* are the PPa in zebrafish, homologous to the mouse PVN. (Scale bars, 200 μm.) (*E*) Representative photomicrograph of the Cre-dependent TdTomato in the PVN CRH neurons. (Magnification: *E*, 10×.) (*F*) Representative voltage-clamp traces of sIPSCs in response to SAM2 application in PVN CRH neurons. (*G*) SAM2 application significantly increased sIPSC frequency. (*H*) SAM2 did not affect sIPSC amplitude. (*I*) Representative voltage-clamp trace of eIPSC onto CRH neurons in response to SAM2 application. (*J*) SAM2 did not affect the amplitude of eIPSCs. (*K*) SAM2 did not change the paired-pulse ratio. *$P < 0.05$; **$P < 0.01$.

distance) compared with wild-type. Also notably, novelty-induced increase of shoaling remained persistently elevated in the null mutants, whereas it showed the expected normal habituation (time-dependent reduction) in wild-type control fish (Fig. 4). Consistent with these findings, our *Sam2* KO mice also exhibited increased anxiety-like responses, for example, on the elevated plus maze (Fig. 5*C*).

In addition to the elevated anxiety-like and fear responses in our null mutant zebrafish, we found an increase in *crhb* mRNA expression in the hypothalamus. CRH neurons are under constant GABAergic suppression in vivo (53), but importantly, our experimental manipulation (i.e., bath application of SAM2) increased sIPSC frequency. These data indicate that SAM2 plays a role in tonic GABAergic suppression of CRH excitability, which may, at least in part, be responsible for the elevated anxiety-like responses observed in both KO models. It is also worth considering that the downstream effects of CRH and the resulting release of glucocorticoids may also contribute to the anxiety phenotype (14, 54).

Identification of the specific neural circuits mediating the effects of SAM2 first requires the determination of neuronal cell types or neurotransmitter systems involved. In case of glucocorticoid receptors, their actions on fear and anxiety behaviors have recently been shown to be mediated via glutamatergic but not GABAergic neural circuits in the mouse forebrain (45). We performed in situ hybridization analysis with GABAergic, glutamatergic, and *sam2* markers in the adult fish brain to determine colocalization. *sam2* expression within the Vd, Vc, Hc, and Hd was found to be predominantly confined to *GAD65/67*$^{+}$ GABAergic neurons, whereas expression in the Dm revealed colocalization with *vglut2b*$^{+}$ glutamatergic neurons. Whether *sam2*-expressing neurons employ GABA or glutamate as a second transmitter remains to be determined (55). Also, whether *sam2* regulates the neuronal activity of GABAergic or glutamatergic neurons by neuromodulatory action will need to be ascertained in the future. Nevertheless, the expression and colocalization patterns reported in our current study open the possibility of a neuromodulatory role of *sam2* in both excitatory and inhibitory neurotransmitter systems comprising anxiety circuitry.

The specific molecular mechanisms underlying increased anxiety-like behavioral responses observed in *sam2* KO fish will require further characterization. Nevertheless, the behavioral

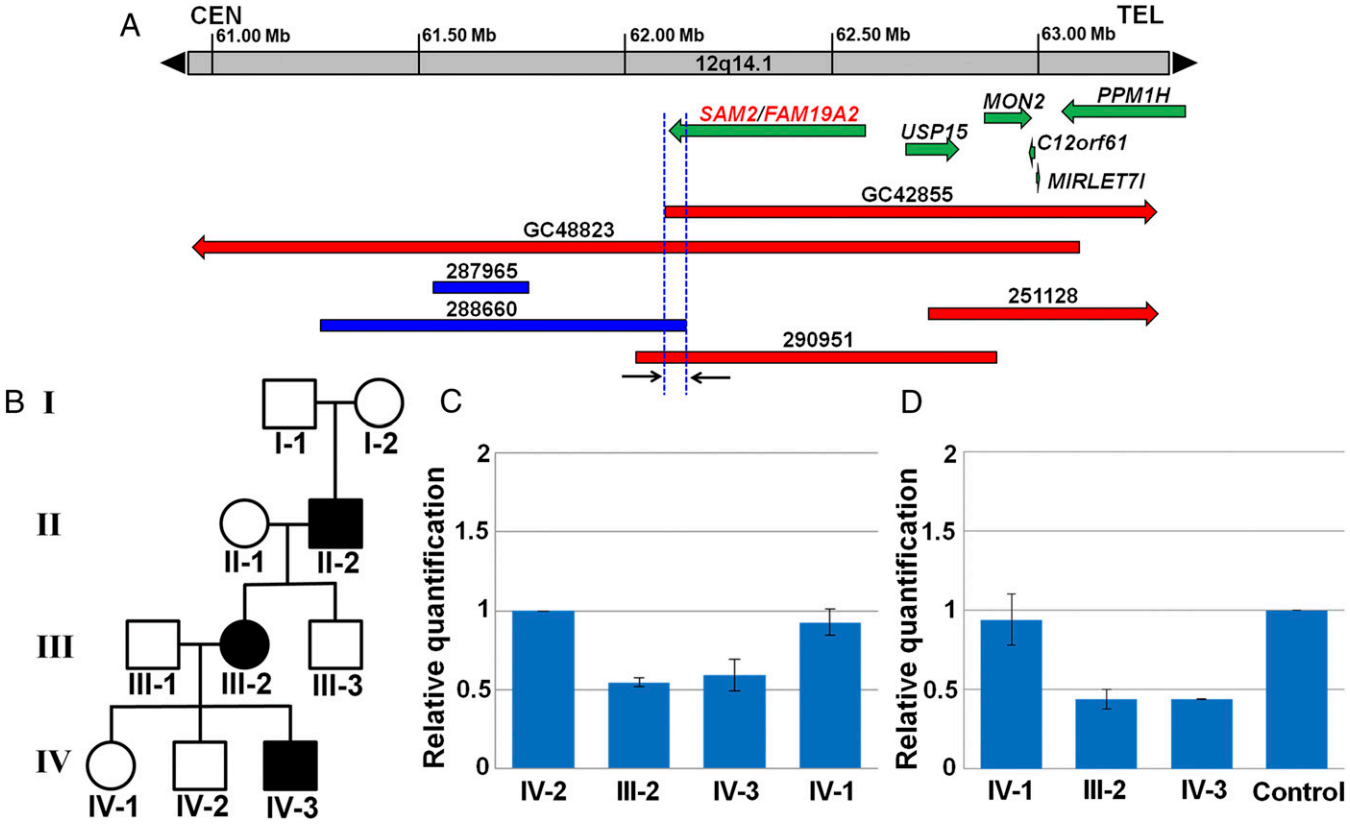

Fig. 7. CNV mapping at 12q14.1 with six human patients, implicating *SAM2* as a candidate gene. Deletions and duplications are depicted in red and blue, respectively. (*A*) Alignment of three microdeletions and one microduplication at 12q14.1 has refined the candidate gene region to a 61 kb (arrows), which contains 56-kb 3′ end of *SAM2*. Notably, the microdeletion in a 6-y-old boy 290951 with autism spectrum disorder and intellectual disability contains *SAM2*, as well as *USP15* and part of *MON2*. (*B*) Pedigree showing three family members affected by intellectual disability in three generations. We have confirmed the deletion in each family member; II-2 (del/+), III-2 (del/+), III-3 ($^{+/+}$), IV-1 ($^{+/+}$), IV-2 ($^{+/+}$), and IV-3 (del/+). (*C*) *SAM2* copy number in the family as determined by qPCR. The proband IV-3 has inherited the deletion from the maternal grandfather II-2 through his mother III-2 and affected members have only one *SAM2* copy. The patient's siblings are normal having two *SAM2* copies. (*D*) Transcript levels of *SAM2* in patient, his mother, sister, and white male control as revealed by qRT-qPCR. *SAM2* transcripts are reduced approximately by half in both the patient and his mother relative to control.

changes we found appeared to be unrelated to the serotonergic neurotransmitter system, as the expression of indicative markers, such as *tphR* and *slc6a4a*, were not affected by the loss of *sam2* (*SI Appendix*, Fig. S6 *P*–*Q*′) (29, 56). However, after the novel tank assays, *sam2* KO fish did show higher level of *c-fos* expression in the entire brain compared with wild-type (*SI Appendix*, Fig. S6 *S* and *S*′), confirming their abnormal response to novelty but also implying potential involvement of neurotransmitters other than the glutamatergic and GABAergic systems.

Finally, comparative genomic mapping with microdeletions and microduplications in human patients with intellectual disability, autism, and behavioral tantrums has identified *SAM2* as a candidate gene for these phenotypes in individuals with 12q14.1 CNVs (Fig. 7). Although the latter results do not prove the role of *SAM2* in these diseases, these results, together with our findings with zebrafish and mice, present an interesting possibility: evolutionarily distant species, such as fish, rodents, and humans, may possess similar mechanisms underlying anxiety and emotion, and these mechanisms may include *sam2*. We thus propose that the discovery of the *samdori* gene family and the functional information of one of its member s*am2*, may have important translational relevance and therapeutic potential.

Materials and Methods

Full methods and any associated references are available in *SI Appendix, SI Materials and Methods*.

Animals. All experimental protocols and procedures were approved and conducted according to the approved guidelines and regulations of the Animal Ethics Committee of Chungnam National University (CNU-00866).

Isolation of *samdori* Gene Family. We established a unique insertional mutagenesis system based on the Sleeping Beauty transposon, called the golden fish project (*SI Appendix*, Fig. S1). In addition to the GFP gene, we used a melanin-concentrating hormone gene as a transgene reporter for visual screening of mutants. During the course of mutagenesis, we mapped the insertion site in a chemokine gene, named *samdori* (*sam*). The full-length cDNAs of zebrafish *sam-1a*, *1b*, *2*, *3a*, *3b*, *4*, *5a*, and *5b* genes were isolated using the RACE technique. The *sam2* KO zebrafish lines ($sam2^{cnu1}$ and $sam2^{cnu2}$) and *Sam2* KO mice were generated by the targeted mutagenesis utilizing ZFNs (26, 27) and transcription activator-like endonucleases (57), respectively.

Behavior Tests in Zebrafish and Mice. Male zebrafish siblings of identical age (3-mo-old) and size were used for the following behavioral tests: open novel tank (35, 36, 41), scototaxis (37), and shoaling behavior (1, 42). The open-field test, elevated plus maze, and fear conditioning were employed in mice. All values represent mean ± SEM.

Human Genetics Data. Patients GC42855 and GC48823 were identified among a cohort of ∼32,700 patients undergoing clinical, oligonucleotide-based array comparative genomic hybridization (aCGH) (58, 59) at Signature Genomic Laboratories. The DECIPHER database is a publicly accessible web-based resource of human genome variants with associated phenotypes, which facilitates the identification and interpretation of pathogenic genetic variation in thousands of patients with rare disorders worldwide (47). The description of case 290951 was ascertained from the DECIPHER database.

We tested the deletion in 290951 family members; II-2 (affected, has deletion), III-2 (mother, affected, has deletion), III-3 (uncle, unaffected, does not have deletion), IV-1 (elder sister, unaffected, no deletion), IV-2 (elder brother, unaffected, no deletion), IV-3 (the proband, affected, has the deletion). This study was approved by the Institutional Review Board of Augusta University, Augusta, Georgia (HAC 0904264) for collection of deidentified phenotypic and genotypic data of human subjects or, with informed consent, for additional studies completed on blood or DNA. Informed consent, blood, and cells, were obtained from the family of 290951, while deidentified data were used for the rest of the analyses.

ACKNOWLEDGMENTS. We thank Ted Inpyo Hong, Soojin Ryu, and Cecilia Hillard for proofreading and critical review of the manuscript. This study makes use of data generated by the DECIPHER community. A full list of centers who contributed to the generation of the data is available from https://decipher.sanger.ac.uk and via email from decipher@sanger.ac.uk. This work was supported by Ministry of Trade, Industry and Energy, Korea Grant 10063396; the National Research Foundation of Korea Grants 2017R1A2B2010696 and 2017M3A9A5051180; Institute for Basic Science Grants IBS-R001-D1 and IBS-R021; and a Natural Sciences and Engineering Research Council grant (to R.G.).

1. Gerlai R (2010) Zebrafish antipredatory responses: A future for translational research? *Behav Brain Res* 207:223–231.
2. Patterson B, Van Ameringen M (2016) Augmentationt strategies for treatment-resistant anxiety disorders: A systematic review and meta-analysis. *Depress Anxiety* 33:728–736.
3. Okamoto H, Aizawa H (2013) Fear and anxiety regulation by conserved affective circuits. *Neuron* 78:411–413.
4. Deverman BE, Patterson PH (2009) Cytokines and CNS development. *Neuron* 64: 61–78.
5. Rostène W, Kitabgi P, Parsadaniantz SM (2007) Chemokines: A new class of neuromodulator? *Nat Rev Neurosci* 8:895–903.
6. Réaux-Le Goazigo A, Van Steenwinckel J, Rostène W, Mélik Parsadaniantz S (2013) Current status of chemokines in the adult CNS. *Prog Neurobiol* 104:67–92.
7. Hikosaka O (2010) The habenula: From stress evasion to value-based decision-making. *Nat Rev Neurosci* 11:503–513.
8. Amo R, et al. (2010) Identification of the zebrafish ventral habenula as a homolog of the mammalian lateral habenula. *J Neurosci* 30:1566–1574.
9. Kalueff AV, Stewart AM, Gerlai R (2014) Zebrafish as an emerging model for studying complex brain disorders. *Trends Pharmacol Sci* 35:63–75.
10. Turner KJ, et al. (2016) Afferent connectivity of the zebrafish habenulae. *Front Neural Circuits* 10:30.
11. Zhang BB, Yao YY, Zhang HF, Kawakami K, Du JL (2017) Left habenula mediates light-preference behavior in zebrafish via an asymmetrical visual pathway. *Neuron* 93: 914–928.e4.
12. Kim C-H, et al. (2000) Repressor activity of Headless/Tcf3 is essential for vertebrate head formation. *Nature* 407:913–916.
13. Itoh M, et al. (2003) Mind bomb is a ubiquitin ligase that is essential for efficient activation of Notch signaling by Delta. *Dev Cell* 4:67–82.
14. Ziv L, et al. (2013) An affective disorder in zebrafish with mutation of the glucocorticoid receptor. *Mol Psychiatry* 18:681–691.
15. Tom Tang Y, et al. (2004) TAFA: A novel secreted family with conserved cysteine residues and restricted expression in the brain. *Genomics* 83:727–734.
16. Higashijima S, Mandel G, Fetcho JR (2004) Distribution of prospective glutamatergic, glycinergic, and GABAergic neurons in embryonic and larval zebrafish. *J Comp Neurol* 480:1–18.
17. Bae YK, et al. (2009) Anatomy of zebrafish cerebellum and screen for mutations affecting its development. *Dev Biol* 330:406–426.
18. Gamse JT, et al. (2005) Directional asymmetry of the zebrafish epithalamus guides dorsoventral innervation of the midbrain target. *Development* 132:4869–4881.
19. deCarvalho TN, et al. (2014) Neurotransmitter map of the asymmetric dorsal habenular nuclei of zebrafish. *Genesis* 52:636–655.
20. deCarvalho TN, Akitake CM, Thisse C, Thisse B, Halpern ME (2013) Aversive cues fail to activate fos expression in the asymmetric olfactory-habenula pathway of zebrafish. *Front Neural Circuits* 7:98.
21. Ryu S, Holzschuh J, Mahler J, Driever W (2006) Genetic analysis of dopaminergic system development in zebrafish. *J Neural Transm Suppl* 70:61–66.
22. Unger JL, Glasgow E (2003) Expression of isotocin-neurophysin mRNA in developing zebrafish. *Gene Expr Patterns* 3:105–108.
23. Faraco JH, et al. (2006) Regulation of hypocretin (orexin) expression in embryonic zebrafish. *J Biol Chem* 281:29753–29761.
24. Jesuthasan S (2012) Fear, anxiety, and control in the zebrafish. *Dev Neurobiol* 72: 395–403.
25. Lau BYB, Mathur P, Gould GG, Guo S (2011) Identification of a brain center whose activity discriminates a choice behavior in zebrafish. *Proc Natl Acad Sci USA* 108: 2581–2586.
26. Kim J-S, Lee HJ, Carroll D (2010) Genome editing with modularly assembled zinc-finger nucleases. *Nat Methods* 7:91, author reply 91–92.
27. Foley JE, et al. (2009) Targeted mutagenesis in zebrafish using customized zinc-finger nucleases. *Nat Protoc* 4:1855–1867.
28. Filippi A, et al. (2007) Expression and function of nr4a2, lmx1b, and pitx3 in zebrafish dopaminergic and noradrenergic neuronal development. *BMC Dev Biol* 7:135.
29. Lillesaar C (2011) The serotonergic system in fish. *J Chem Neuroanat* 41:294–308.
30. Doll CA, Burkart JT, Hope KD, Halpern ME, Gamse JT (2011) Subnuclear development of the zebrafish habenular nuclei requires ER translocon function. *Dev Biol* 360:44–57.
31. Berman JR, Skariah G, Maro GS, Mignot E, Mourrain P (2009) Characterization of two melanin-concentrating hormone genes in zebrafish reveals evolutionary and physiological links with the mammalian MCH system. *J Comp Neurol* 517:695–710.
32. Song Y, Golling G, Thacker TL, Cone RD (2003) Agouti-related protein (AGRP) is conserved and regulated by metabolic state in the zebrafish, *Danio rerio*. *Endocrine* 22:257–265.
33. Löhr H, Hammerschmidt M (2011) Zebrafish in endocrine systems: Recent advances and implications for human disease. *Annu Rev Physiol* 73:183–211.
34. Beretta CA, Dross N, Guiterrez-Triana JA, Ryu S, Carl M (2012) Habenula circuit development: Past, present, and future. *Front Neurosci* 6:51.
35. Cachat J, et al. (2010) Measuring behavioral and endocrine responses to novelty stress in adult zebrafish. *Nat Protoc* 5:1786–1799.
36. Stewart A, et al. (2012) Modeling anxiety using adult zebrafish: A conceptual review. *Neuropharmacology* 62:135–143.
37. Maximino C, Marques de Brito T, Dias CA, Gouveia A, Jr, Morato S (2010) Scototaxis as anxiety-like behavior in fish. *Nat Protoc* 5:209–216.
38. Speedie N, Gerlai R (2008) Alarm substance induced behavioral responses in zebrafish (*Danio rerio*). *Behav Brain Res* 188:168–177.
39. Egan RJ, et al. (2009) Understanding behavioral and physiological phenotypes of stress and anxiety in zebrafish. *Behav Brain Res* 205:38–44.
40. Partridge BL, Ptcher T, Cullen JM, Wilson J (1980) The three-dimensional structure fo fish schools. *Behav Ecol Sociobiol* 6:277–288.
41. Wong K, et al. (2010) Analyzing habituation responses to novelty in zebrafish (*Danio rerio*). *Behav Brain Res* 208:450–457.
42. Mahabir S, Chatterjee D, Buske C, Gerlai R (2013) Maturation of shoaling in two zebrafish strains: A behavioral and neurochemical analysis. *Behav Brain Res* 247:1–8.
43. Major P, Dill L (1978) The three-dimensional structure of airborne bird flocks. *Behav Ecol Sociobiol* 4:111–122.
44. Stewart AM, Braubach O, Spitsbergen J, Gerlai R, Kalueff AV (2014) Zebrafish models for translational neuroscience research: From tank to bedside. *Trends Neurosci* 37: 264–278.
45. Hartmann J, et al. (2017) Forebrain glutamatergic, but not GABAergic, neurons mediate anxiogenic effects of the glucocorticoid receptor. *Mol Psychiatry* 22:466–475.
46. Zhang R, et al. (2017) Loss of hypothalamic corticotropin-releasing hormone markedly reduces anxiety behaviors in mice. *Mol Psychiatry* 22:733–744.
47. Firth HV, et al. (2009) DECIPHER: Database of chromosomal imbalance and phenotype in humans using Ensembl resources. *Am J Hum Genet* 84:524–533.
48. Zou Q, et al. (2014) USP15 stabilizes MDM2 to mediate cancer-cell survival and inhibit antitumor T cell responses. *Nat Immunol* 15:562–570.
49. Agetsuma M, et al. (2010) The habenula is crucial for experience-dependent modification of fear responses in zebrafish. *Nat Neurosci* 13:1354–1356.
50. Lee A, et al. (2010) The habenula prevents helpless behavior in larval zebrafish. *Curr Biol* 20:2211–2216.
51. Okamoto H, Agetsuma M, Aizawa H (2012) Genetic dissection of the zebrafish habenula, a possible switching board for selection of behavioral strategy to cope with fear and anxiety. *Dev Neurobiol* 72:386–394.
52. Ganz J, et al. (2014) Subdivisions of the adult zebrafish pallium based on molecular marker analysis. *F1000Res* 3:308.
53. Stratton MS, Searcy BT, Tobet SA (2011) GABA regulates corticotropin releasing hormone levels in the paraventricular nucleus of the hypothalamus in newborn mice. *Physiol Behav* 104:327–333.
54. Griffiths BB, et al. (2012) A zebrafish model of glucocorticoid resistance shows serotonergic modulation of the stress response. *Front Behav Neurosci* 6:68.
55. Filippi A, Mueller T, Driever W (2014) vglut2 and gad expression reveal distinct patterns of dual GABAergic versus glutamatergic cotransmitter phenotypes of dopaminergic and noradrenergic neurons in the zebrafish brain. *J Comp Neurol* 522: 2019–2037.
56. Lillesaar C, Stigloher C, Tannhäuser B, Wullimann MF, Bally-Cuif L (2009) Axonal projections originating from raphe serotonergic neurons in the developing and adult zebrafish, *Danio rerio*, using transgenics to visualize raphe-specific pet1 expression. *J Comp Neurol* 512:158–182.
57. Sung YH, et al. (2013) Knockout mice created by TALEN-mediated gene targeting. *Nat Biotechnol* 31:23–24.
58. Ballif BC, et al. (2008) Identification of a previously unrecognized microdeletion syndrome of 16q11.2q12.2. *Clin Genet* 74:469–475.
59. Duker AL, et al. (2010) Paternally inherited microdeletion at 15q11.2 confirms a significant role for the SNORD116 C/D box snoRNA cluster in Prader-Willi syndrome. *Eur J Hum Genet* 18:1196–1201.

Supporting Information

Choi et al. 10.1073/pnas.1707663115

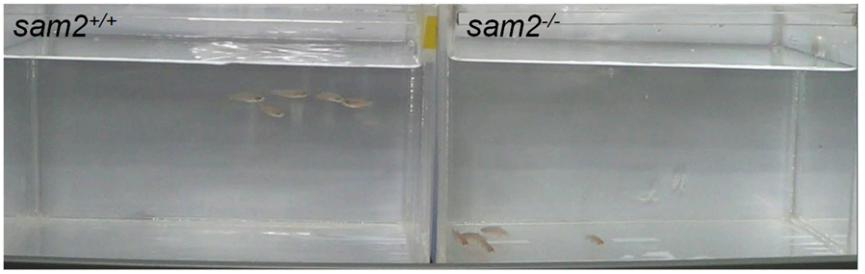

Movie S1. Video record showing anxiety-like behavior and increased social cohesion in *sam2*^{cnu1} KO fish. Five adult fish (3-mo-old male siblings) were placed as a group in a novel tank: (*Left* tank) *sam2*$^{+/+}$ control siblings; (*Right* tank) *sam2*$^{-/-}$ KO siblings. Only a short part of the video recording (40 s) is shown of the 15-min novel tank test. The fish have a tendency to stay on the bottom before habituation to the new environment. Usually, it takes more than 10 min for wild-type fish to adapt to the novel tank. Mutant siblings show typical anxiety behavior and higher aggregation.

Movie S1

Other Supporting Information Files

SI Appendix (PDF)

Supporting information for

Targeted knockout of a novel chemokine-like gene increases anxiety and fear responses

Jung-Hwa Choi, Yun-Mi Jeong, Sujin Kim, Boyoung Lee, Krishan Ariyasiri, Hyun-Taek Kim, Seung-Hyun Jung, Kyu-Seok Hwang, Tae-Ik Choi, Chul O Park, Won-Ki Huh, Matthias Carl, Jill A. Rosenfeld, Salmo Raskin, Alan Ma, Jozef Gecz, Hyung-Goo Kim, Jin-Soo Kim, Ho-Chul Shin, Doo-Sang Park, Robert Gerlai, Bradley B. Jamieson, Joon S. Kim, Karl J. Iremonger, Sang H. Lee, Hee-Sup Shin*, and Cheol-Hee Kim*

*Corresponding authors, E-mail**:** zebrakim@cnu.ac.kr, shin@ibs.re.kr

SI Materials and Methods

Animals. *Zebrafish:* Wild-type zebrafish (*Danio rerio*), and *Et(-1otpa::mmGFP)hd1* enhancer trap transgenic fish (1) were raised and maintained under standard condition at 28.5 ˚C. Embryos were fixed at specific stages as described previously (2). All experimental protocols and procedures were approved and conducted according to the approved guidelines and regulations of the Animal Ethics Committee of Chungnam National University).

Mouse: (Behavior) Animal care and experimental procedures followed the guidelines of the Institutional Animal Care and Use Committee of the Institute of Basic Science. Experiments were performed with male C57BL/6N mice (8-14 weeks of age). Mice were housed in groups of four or five with free access to food and water, under controlled temperature and light conditions (23 ℃, 12-h light: 12-h dark cycle). Experiments were performed during the light phase.

Mouse: (Brain slice electrophysiology) Adult male mouse Crh-IRES-Cre; Ai14 (TdTomato) were group housed in controlled temperature (20 ± 2 ºC) and lighting (12-h light, 12-h dark) conditions with ad libitum access to food and water. Mouse experimental procedures were approved by the University of Otago Animal Ethics Committee.

The golden fish project. After conducting a genetic screen, the mapping of chemically induced mutants is difficult due to high cost and labor. Insertional mutagenesis is an alternative approach to chemical mutagenesis which speeds up the identification of mutated genes (3, 4). Using this approach, we established a unique insertional mutagenesis system based on the Sleeping Beauty transposon (4). In addition to the green fluorescent protein (GFP) gene, we introduced a melanin-concentrating hormone (MCH) gene as a transgene reporter in our insertional mutagenesis. MCH was originally isolated from the pituitary gland of fish where it controls skin pigmentation. Enhanced expression of MCH in transgenic medaka fish

can induce melanosome aggregation and change body color into albino or “golden” (5). Although GFP reporter can be monitored under fluorescent microscopy in live zebrafish embryos, however, it is not easy to detect the signal which is expressed in small subsets of cells in a specific tissue in adult zebrafish. This lack of GFP fluorescent penetration in adult zebrafish could be overcome by using our dual reporter system; GFP plus MCH. After visual screening of mutants with GFP fluorescence and melanosome aggregation, mapping of the insertion site was performed using the DNA walking Speedup kit (Cat. K1052, Seegene, Seoul. Korea)

Isolation of *samdori* gene family. After screening and mapping of insertional mutants, we discovered a novel chemokine gene, named *samdori (sam)* which means the third son in Korean (Fig. S1). From the NCBI database we further identified the existence of total eight members of this *sam* gene family in the zebrafish genome. Since there were five *SAM* genes in mammals, we named them as *sam-1a, -1b, 2, 3a, -3b, 4, 5a,* and *5b,* respectively.

Cloning of zebrafish *samdori* gene family. The full-length cDNAs of zebrafish *sam-1a, 2, 3b, 4, 5a, 5b* genes were isolated using the 5’-, 3’-RACE (Rapid Amplification of cDNA ends) technique (FirstChoice RLMRACE Kit, Ambion). Primers used: *sam-1a*, 5’-CAGCCGGTGCTCCTGCCATGTCCTGGCTC-3’ for forward, 5’-GGAGCTCTTTGTTAGGTCCGGGGATGA-3’ for reverse; *sam-1b*, 5’-CGATACAGAGGAGTGTTGGGATGTCGTGG-3’ for forward, 5’-GCAGTGATTCTACCTCTGCTACAAGGA-3’ for reverse; *sam-2*, 5’-ACGCCGCTGAATGAACCGATTACCGG-3’ for forward, 5’-GAGCGAACGCACTGCTTTACACAC-3’ for reverse; *sam-3a*, 5’-CAGCTCAACGAGGGGGATGCGGGAGAGG-3’ for forward, 5’-GGTCCCAGACTATCGTGTGACCTTGGTC-3’ for reverse; *sam-3b*, 5’-

ACTACCGCGCCAACAGGATGCA-3' for forward, 5'-GTCCTGGGACAAAAGAGCTGA-3' for reverse; *sam-4*, 5'-GCTCGTTTAAAACAAACATCTGTCTTCAGGAC-3' for forward, 5'-GAACTGCCATGTTGTTGCTATCGTGTGACC-3' for reverse; *sam-5a*, 5'-GGAGATGTGGCGTGGATGCTGAAGGCAG-3' for forward, 5'-CCTCCCACTGTTAGGACACCGTTGTAGT-3' for reverse; *sam-5b*, 5'-ACGCGTCAGATCCTCGGAAAGATGCAGC-3' for forward, 5'-CCACTGGCGTCAGGATACCGTGGTTGT-3' for reverse.

Whole-mount *in situ* hybridization. Whole-mount *in situ* hybridization and two-color *in situ* hybridization were performed as described previously with some modifications. RNA probes for *aoc1, agrp, c-fos, crhb, cxcr4b, dat, fam84b, gad1b, gad2, hcrt, lov, mch, npy, otx5, oxt (itnp), pet-1, sst1, th, tphR, vglut2a, vglut2b,* and *sam2* gene, were synthesized using SP6, T7 or T3 RNA polymerase. For two-color *in situ* hybridization, fluorescein-labeled riboprobes were synthesized as described previously (6, 7).

Immunohistochemistry. Whole-mount immunostaining was performed as described previously (8). Fixed embryos were permeabilized with 10 μg/ml Proteinase K for 30 min and re-fixed with 4% paraformaldehyde in PBST for 20 min. The embryos were incubated with the primary and secondary antibody overnight. Antibodies used were rabbit-anti-5HT (ImmunoStar; 1:100), and goat-anti-rabbit Alexa Flour 488 (LifeTechnologies; 1:500).

Paraffin and frozen section. After whole-mount *in situ* hybridization, embryos were dehydrated by a graded series of ethanol treatments. Dehydrated embryos were transferred to xylene and soaked in paraffin overnight. After embedding, sections were cut at 5 μm thickness (9). In the case of frozen section, stained tissues were washed with PBS and cryoprotected in 30% sucrose/PBS (wt/vol) overnight at 4 ˚C. Tissues were embedded in

frozen section compounds (FSS 22, Leica Microsystems) and cryosectioned to 12- 20 µm (10).

Generation of zebrafish *sam2* and mouse *Sam2* KO mutants. *Zebrafish*: Target specific ZFN vectors for *sam2* were designed and synthesized, as previously described (11). ZFN vectors were linearized with *Pvu*II and capped mRNAs were synthesized using T7 RNA polymerase. Two to three nanograms of ZFN mRNA was injected into one cell stage embryos. For identification and genotyping of *sam2* KO fish, we used the *T7 endonuclease 1* (*T7E1*; New England Biolabs) assay to detect heteroduplex formation after DNA denaturation and annealing. Primers used for *sam2*^{cnu1} genotyping were *sam2*^{cnu1} forward (5'-TCTACTGAGGAGTGGTGTGA-3') and *sam2*^{cnu1} reverse (5'-GGTCAGTTTCAGAGAGCTGG-3'), respectively. Primers used for *sam2*^{cnu2} genotyping were *sam2*^{cnu2} forward (5'-AGACCGTCAAGTGCTCCTGC-3') and *sam2*^{cnu2} reverse (5'-GGTCAGTTTCAGAGAGCTGG-3'), respectively.

Mouse: TALEN vectors were linearized with *PvuII* and capped mRNAs were synthesized using T7 RNA polymerase. The pair of TALEN mRNA was injected into the cytoplasm of fertilized eggs. TALEN-mediated *Sam2* F0 mice were screened by *T7E1* assay as we previously described (12). The genomic DNA was prepared from tail biopsies and amplified using TALEN target site primers. Founder line #15 (14 bp-deletion) was backcrossed with C57BL/6N and heterozygous breeding was set up to generate *Sam2* KO mice (*Sam2*$^{-/-}$). Primers used for genotyping were mouse *Sam2* forward (5'-GTGAGAAATTCAGTGTTCTGGG-3') and mouse *Sam2* reverse (5'-CCTGAAGACAGCTCTCTGCA-3'). Further, PCR products were digested with *BslI* restriction enzyme to confirm the deleted sequence in mutant mouse.

Open tank test, scototaxis test and thigmotaxis test in zebrafish. To measure anxiety-like behavior, male zebrafish siblings of

identical age and size (3 to 3.5 cm) were tested. Fish were placed into the novel open tank (15 cm × 15 cm × 25 cm; height × width × length) for 10 min and their movements were recorded with a video camera (13, 14). Open tank test was repeated eighteen times for control and twenty eight times for the *sam2*^{cnu1} allele. For the scototaxis test, we measured the preference of black vs. white compartments. Individual fish was placed into a tank coated with black and white plastic sheet and allowed to acclimate for 5 min and then monitored by video recording for 15 min (15, 16). Scototaxis test was repeated eighteen times for control and twenty four times for the *sam2*^{cnu1} allele. For the thigmotaxis, we placed six-male fish in the tank (15 cm × 15 cm × 25 cm; height × width × length) for 30 min and measured the time spent in the corner (one fifth of tank's left and right parts) and the center (rest of corner of the tank) every one minute. The experiment was repeated twelve times of both the control and *sam2*^{cnu1} allele. EthoVision XT7 (Noldus Info Tech, Wageningen, The Netherlands) was used to analyze fish behavior. To track a single fish, we selected the "difference" in steps of the detection setting of Ethovision (16).

Alarm substance assay (skin extract)

Alarm substance was freshly prepared by making 10-15 shallow lesions on both side of the zebrafish skin using a sharp razor. Seven fish were immersed in 50 ml of 20 mM Tris-Cl (pH 8.0) for 25 seconds and filtered using a 0.2 μm filter (Sartorius stedim, 16534). To test alarm response, five three-month-old fish were placed in tank containing 4 liters of aquarium water. After acclimated fish in the aquarium water for 30 minutes, gently added 10 ml of alarm substance into the surface of the water (17, 18).

Three-dimensional reconstruction of swim path and fish positions. Fish position (x and y coordinates from the dorsal view and z coordinates from frontal view) was recorded at 20 sec intervals for the early phase recording (5-8 min) and the late phase recording (13-16 min) time based on our preliminary data. Inter-fish distances or individual gaps (measured between

the focal fish and its shoal mates) were calculated using the (distance= $\sqrt{(x_a - x_0)^2 + (y_a - y_0)^2 + (z_a - z_0)^2}$) where x_0, y_0 and z_0 were x, y and z coordinates of the focal fish while x_a, y_a and z_a represent coordinates of shoal member at the defined time (19, 20). Meanwhile x, y and z coordinates of the core fish were considered as the zero point of in the shoal at the defined time. Cohesion experiment was repeated three times in the *sam2*^{cnu1} and twice in the *sam2*^{cnu2} allele. Both alleles showed similar results. For statistical analysis SigmaPlot (Version 10, SigmaPlot, Chicago, IL, USA) was used. The effect size (Cohen's *d*) was calculated for the social cohesion of control and KO fish at early and late phases.

Open field test in mice. The open field chamber consisted of a 40 cm (W) x 40 cm (L) x 40 cm (H) white acrylic box. Mice were placed in one of the four corners of the open field and allowed to explore the chamber for 30 min. The field was illuminated at 10 lux. Total distance moved for 30 min was recorded for each mouse. After the test, each mouse was returned to its home cage and the box was wiped clean using 70% ethanol and distilled water. Activity was monitored and analyzed on Ethovision 9.0 (Noldus Information Technologies, Leesburg, VA). Each behavior test was performed with one-week interval. Behavior results were obtained from at least three different batches of animals.

Elevated plus maze. Custom made mouse elevated plus maze was made of grey acrylic base and consisted of four arms (two cross-shaped arms (length: 30 cm, width: 5 cm, height from floor: 40 cm). Two arms (closed arms) were enclosed with 15-cm high walls and the other two (open arms) were not. The enclosed arms and the open arms faced each other on opposite sides. For the test, mice were placed in the center square and allowed to move freely for five minutes. Open arm entries were defined as the mouse having all four paws onto the open arm. Time spent in open arms (%; [time in open

arms] / [time in closed arms + time in open arms] x100) was analyzed to measure anxiety. Behavior was monitored and analyzed on Ethovision 9.0 (Noldus Information Technologies, Leesburg, VA).

Fear conditioning. Fear conditioning was performed as previously described with minor modifications (21). For the training, mice were placed in the fear conditioning chamber (context A) for 3 min, and then mice were received paired stimuli of tone (30 s, 86 dB, 3000 Hz) and a co-terminating shock (1 s, 0.7 mA). Mice underwent a total of four conditioned stimulus-unconditioned stimulus (CS-US) pairs separated by 120-sec intervals. Twenty-four hours after training, contextual fear memory was tested in the same chamber (context A) for 5 mins in the absence of the auditory stimulus and shock. After 3 hrs, cued fear memory was tested in a different context (context B: novel chamber, odor, floor, and visual cues). After 10 min of exploration time, the 30-sec auditory CS was delivered. The freezing of the mice was recorded and analyzed with FreezeFrame software (Actimetrics, Wilmette, IL).

RT-PCR analysis of mouse *Sam2* expression

For reverse transcription-polymerase chain reaction (RT-PCR) analysis, mice were euthanized and brains were isolated and immediately frozen on dry ice. Frozen brains were stored at -80 °C prior to cryosectioning. The next day, the brains were cryosectioned at a thickness of 250 μm. Frozen sliced brain tissue was collected on cold slide glass and dissected under a microscope. Total RNAs from each brain tissue of wild-type mice were extracted using GeneAll Hybrid-R (GeneAll Biotechnology, Korea). cDNA was synthesized following manufacturer protocol (SuperScript IV VILO Master Mix, Invitrogen). Primers used for RT-PCR were *Sam2* forward (5'-TTCCAGATCGCAAAGGATGG-3') and *Sam2* reverse (5'-AGTCTTCAGGACCCAACGTT-3'), respectively. Primers used for the endogenous control were *Actb* forward (5'-CGGGCTGTATTCCCCTCCATCG-3') and *Actb* reverse (5'-

TGGTGAAGCTGTAGCCACGCTC-3'), respectively.

Preparation of highly purified SAM2 protein

Mammalian SAM2 (residues 31-134, except for the signal peptide) fused to the C-terminal of Protein G was cloned into the modified pX vector (22, 23). This recombinant protein was expressed by transient transfection using PEI in human embryonic kidney 293 EBNA1 (HEK 293E) cells. Transfected HEK 293E cells were grown in suspension for 72 hours at 33 °C. The cells were sonicated in buffer containing 50 mM Tris-HCl (pH 7.5), 200 mM NaCl and 0.5 mM 1,4-Dithiothreitol. The SAM2 protein was prepared by on-column cleavage with PreScission protease. For high purity protein production, the eluted protein was further purified on HiTrap Q HP column (GE Healthcare) operated with a linear NaCl gradient (50-500 mM) with 20 mM Tris-HCl (pH 7.5) and 0.5 mM 1,4-Dithiothreitol, and on HiLoad 26/600 Superdex 75 pg gel filtration column (GE Healthcare) in buffer containing 20 mM Tris-HCl (pH 7.5), 100 mM NaCl and 0.5 mM 1,4-Dithiothreitol. The purity and molecular weight (~12 kDa) of the purified SAM2 protein was confirmed by 10% Tris-tricine-SDS-PAGE analysis, using the protein size marker (Xpert 2 Prestained Protein Marker, 7 to 240 kDa, GenDEPOT) (Fig. S12).

Brain slice electrophysiology. Acute 200 µm coronal brain slices containing the PVN were cut using a vibratome (VT 1200S) and left to recover in 30 ºC artificial cerebrospinal fluid (ACSF) containing (in mM): 126 NaCl, 2.5 KCl, 26 NaHCO3. 1.25 NaH2PO4, 2.5 CaCl2, 1.5 MgCl2 and 10 glucose, saturated in 95% CO_2/5% O_2. Whole-cell patch-clamp recordings were made from tdTomato-fluorescent CRH neurons visualized under an upright microscope (Olympus). Whole-cell patches were made using borosilicate glass electrodes (tip resistance: 2-5 MΩ) filled with an internal solution of (in mM): 130 KCl, 10 HEPES, 0.2 Na2-GTP, 2 Mg2-ATP, adjusted to pH 7.2 with KCl, and to 290 mosM with sucrose. Neurons were voltage clamped at -60 mV. Evoked currents (100 µA) were made in the surrounding PVN tissue using

a monopolar ACSF-filled glass stimulating electrode. Currents were recorded in the presence of CNQX (10 µM). Signals were acquired using a Multiclamp 700B amplifier (Molecular Devices) connected to a Digidata 1440a, and filtered at 2 kHz before digitizing at 10 kHz. Currents were analyzed using Clampfit (Molecular Devices) or MiniAnalysis (Synaptosoft).

Oligonucleotide-based aCGH. Microarray-based comparative genomic hybridization (aCGH) was performed using custom-designed, oligonucleotide-based whole-genome microarray, either 105K (for GC42855, SignatureChipOS version 1.1, manufactured by Agilent, Santa Clara, CA) or 135K (for GC48823, SignatureChipOS version 2.0, manufactured by Roche NimbleGen, Madison, WI), according to previously described methods (24, 25).

Fluorescence *in situ* hybridization (FISH) analysis. Deletions were confirmed and visualized via metaphase FISH analysis using either RP11-22B1 from 12q14.3 (GC42855) or RP11-76L1 from 12q14.1 (GC48823), according to previously described methods (26).

Statistical Analysis. Analysis was performed on appropriate data sets to ascertain normal distribution by calculating Kurtosis and Skewness values. All values represent mean ± standard error of mean (S.E.M.). Statistical significance for the pair was analyzed by the Mann-Whitney *U* test and Student's *t* test (unpaired, two tailed, assuming unequal variance), unless otherwise indicated. Effect size measures for two independent groups by Cohen's *d*. ANOVA with Tukey's *post hoc* test were used for group comparisons. Statistical significance was depicted as follows n.s. (non-significant, $P > 0.05$), *$P<0.05$, **$P<0.01$, and ***$P<0.001$.

Case presentation. Query of Signature's database of abnormalities revealed two overlapping microdeletions (GC42855 and GC48823) at 12q14.1. GC42855 is 6 years-old girl with postnatal failure to thrive (weight and height in the third percentile), developmental delay, large fontanel, clinodactyly, café au lait

spots, scoliosis, osteopenia, temper tantrums, and excessive fear for being alone and heights. GC48823 is 4 years-old girl with autism and seizures. A child 251128 has behavioral problems and intellectual disability and 287965 had global development delay. 288660 has ADHD, autism spectrum disorder, and generalized joint laxity. No additional follow-up clinical information was available for these five individuals.

290951 is a 6 year-old boy, assessed at the age of 5 in clinical genetics with a history of global mild developmental delay, severe speech and language delay, autism spectrum disorder, and significant family history of intellectual disability. He had poor sucking and reflux as baby, requiring speech pathology input for initial bottle feeding. He did not start walking or talking until around the age of 2. He also had quite significant reflux and a number of ‘blue’ episodes as a baby. Developmental problems were also picked up at preschool and he had a full developmental assessment in 2013 which diagnosed him with mild global developmental delay and autism. Griffiths Assessment at the age of 4 years 11 months showed mild developmental delay in overall 2 year 9 month to 3 year 3 month age range with:

- Locomotor : 3-3.5 year equivalent
- Social: 3-3.5 year
- Language: 3-3.5 year
- Hand eye coordination: 2.75-3.25 year
- Performance: 2.25-2.75 years
- Practical reasoning: 2.75-3.25 year
- Language: simple 4-5 word sentences

He was also found to have dysfunction in social participation, planning and ideas and sensory processing issues with touch avoidance and sensory overload. He had inconsistent unusual eye gaze, echolalia, tangential speech, social difficulties, lack of pretend play, meltdowns, restricted behaviour and sensory issues consistent with autism spectrum disorder. At the moment he still has problems with sleep disruption with difficulty initiating sleep and early waking. He also occasionally gets constipated. He has a good appetite and is otherwise healthy.

For his inattention at school, he was started on Ritalin (methylphenidate) and parents noticed significant difference in his attention, behaviour and socialisation. The school have also noticed the same. He is in kindergarten in a support class with five other children and the teachers are very pleased with how he has progressed after starting on stimulant medication. The family have also had significant problems with his behaviour. He does not follow commands well and has episodes where he will cry incessantly and have melt-downs. He also exhibits recurrent self-stimulating hand movement such as pill rolling, flapping as well as repetitive gustatory movements. They have never noticed any seizure activity, regression, or any other abnormal movements.

On examination at 5 years he weighs 17.7 kg (25^{th} centile), his height is 113 cm (50^{th} centile) and head circumference 49.7 cm (2^{nd}-50^{th} centile). He has quite a long face with a broad forehead, light blue eyes, very crowed teeth and a high arched palate. He has a long pronounced chin and also very long cupped ears with very fleshy ear lobes with a horizontal crease across the lobes. His cardiovascular examination was normal as were his genitalia. He has no birth marks. His measurements were:
Inner canthal 2.5 cm, outer canthal 8.5 cm, interpupillary 5.5 cm, palm length 6.8 cm, mid finger length 5 cm. Left hand had single palmar crease and ears were 6.5cm long. Multisequence multiplanar MRI study of the brain has been performed before and after contrast. The ventricles and cerebral sulci outline normally. There is no focal abnormality seen within the grey or white matter. There is no evidence of mesial temporal sclerosis or mass lesion is identified. No evidence of neuronal migrational disorder. No abnormal enhancement identified. The extra-cerebral spaces have a normal appearance. *MRI studies of the brain* had normal findings.

References

1. Beretta CA, Dross N, Gutierrez-Triana JA, Ryu S, & Carl M (2012) Habenula circuit development: past, present and future. *Frontiers in neuroscience* 6.
2. Kimmel CB, Ballard WW, Kimmel SR, Ullmann B, & Schilling TF (1995) Stages of embryonic development of the zebrafish. *Developmental Dynamics* 203(3):253-310.
3. Kawakami K (2005) Transposon tools and methods in zebrafish. *Dev Dyn* 234(2):244-254.
4. Balciunas D, *et al.* (2004) Enhancer trapping in zebrafish using the Sleeping Beauty transposon. *BMC genomics* 5(1):62.
5. Kinoshita M, *et al.* (2001) Transgenic Medaka Overexpressing a Melanin-Concentrating Hormone Exhibit Lightened Body Color but No Remarkable Abnormality. *Marine Biotechnology* 3(6):536-543.
6. Thisse C, Thisse B, Schilling TF, & Postlethwait JH (1993) Structure of the zebrafish snail1 gene and its expression in wild-type, spadetail and no tail mutant embryos. *Development* 119(4):1203-1215.
7. Hauptmann. G & Gerster. T (1994) Two-color whole-mount in situ hybridization to vertebrate and Drosophila embryos. *Trends in Genetics* 10(8):266.
8. McLean DL & Fetcho JR (2004) Ontogeny and innervation patterns of dopaminergic, noradrenergic, and serotonergic neurons in larval zebrafish. *The Journal of comparative neurology* 480(1):38-56.
9. Kim H-T, *et al.* (2008) Isolation and expression analysis of Alzheimer's disease–related gene xb51 in zebrafish. *Developmental Dynamics* 237(12):3921-3926.
10. Lau BYB, Mathur P, Gould GG, & Guo S (2011) Identification of a brain center whose activity discriminates a choice behavior in zebrafish. *Proceedings of the National Academy of Sciences* 108(6):2581-2586.
11. Foley JE, *et al.* (2009) Targeted mutagenesis in zebrafish using customized zinc-finger nucleases. *Nat. Protocols* 4(12):1855-1868.
12. Sung YH, *et al.* (2013) Knockout mice created by TALEN-mediated gene targeting. *Nat Biotechnol* 31(1):23-24.
13. Cachat J, *et al.* (2010) Measuring behavioral and endocrine responses to novelty stress in adult zebrafish. *Nat. Protocols* 5(11):1786-1799.
14. Stewart A, *et al.* (2012) Modeling anxiety using adult zebrafish: A conceptual review. *Neuropharmacology* 62(1):135-143.
15. Maximino C, Marques de Brito T, Dias CAGdM, Gouveia A, & Morato S (2010) Scototaxis as anxiety-like behavior in fish. *Nat. Protocols* 5(2):209-216.
16. Cachat J, *et al.* (2013) Unique and potent effects of acute ibogaine on zebrafish: The developing utility of novel aquatic models for hallucinogenic drug research. *Behavioural brain research* 236(0):258-269.
17. Mathuru Ajay S, *et al.* (2012) Chondroitin Fragments Are Odorants that Trigger Fear Behavior in Fish. *Current Biology* 22(6):538-544.
18. Decarvalho TN, Akitake CM, Thisse C, Thisse B, & Halpern ME (2013) Aversive cues fail to activate fos expression in the asymmetric olfactory-habenula pathway of zebrafish. *Frontiers in Neural Circuits* 7.
19. Wong K, *et al.* (2010) Analyzing habituation responses to novelty in zebrafish (Danio rerio). *Behavioural brain research* 208(2):450-457.
20. Major P & Dill L (1978) The three-dimensional structure of airborne bird flocks. *Behav. Ecol. Sociobiol.* 4(2):111-122.
21. Jeon D KS, Chetana M, Jo D, Ruley HE, Lin SY, Rabah D, Kinet JP, Shin HS. (2010) Observational fear learning involves affective pain system and Cav1.2 Ca2+ channels in ACC. *Nat Neurosci.* .
22. Nguyen Tuan A, *et al.* (Functional Anatomy of the Human Microprocessor. *Cell* 161(6):1374-1387.
23. Backliwal G HM, Chenuet S, Wulhfard S, De Jesus M, Wurm FM. (2008) Rational vector design and multi-pathway modulation of HEK 293E cells yield recombinant antibody titers exceeding 1 g/l by transient transfection under serum-free conditions. *Nucleic Acids Res.* .
24. Ballif BC, *et al.* (2008) Identification of a previously unrecognized microdeletion syndrome of 16q11.2q12.2. *Clinical Genetics* 74(5):469-475.
25. Duker AL, *et al.* (2010) Paternally inherited microdeletion at 15q11.2 confirms a significant role for the SNORD116 C/D box snoRNA cluster in Prader-Willi syndrome. *Eur J Hum Genet* 18(11):1196-1201.
26. Traylor R, *et al.* (2009) Microdeletion of 6q16.1 encompassing EPHA7 in a child with mild neurological abnormalities and dysmorphic features: case report. *Molecular Cytogenetics* 2(1):17.

Supplementary Video and Figures

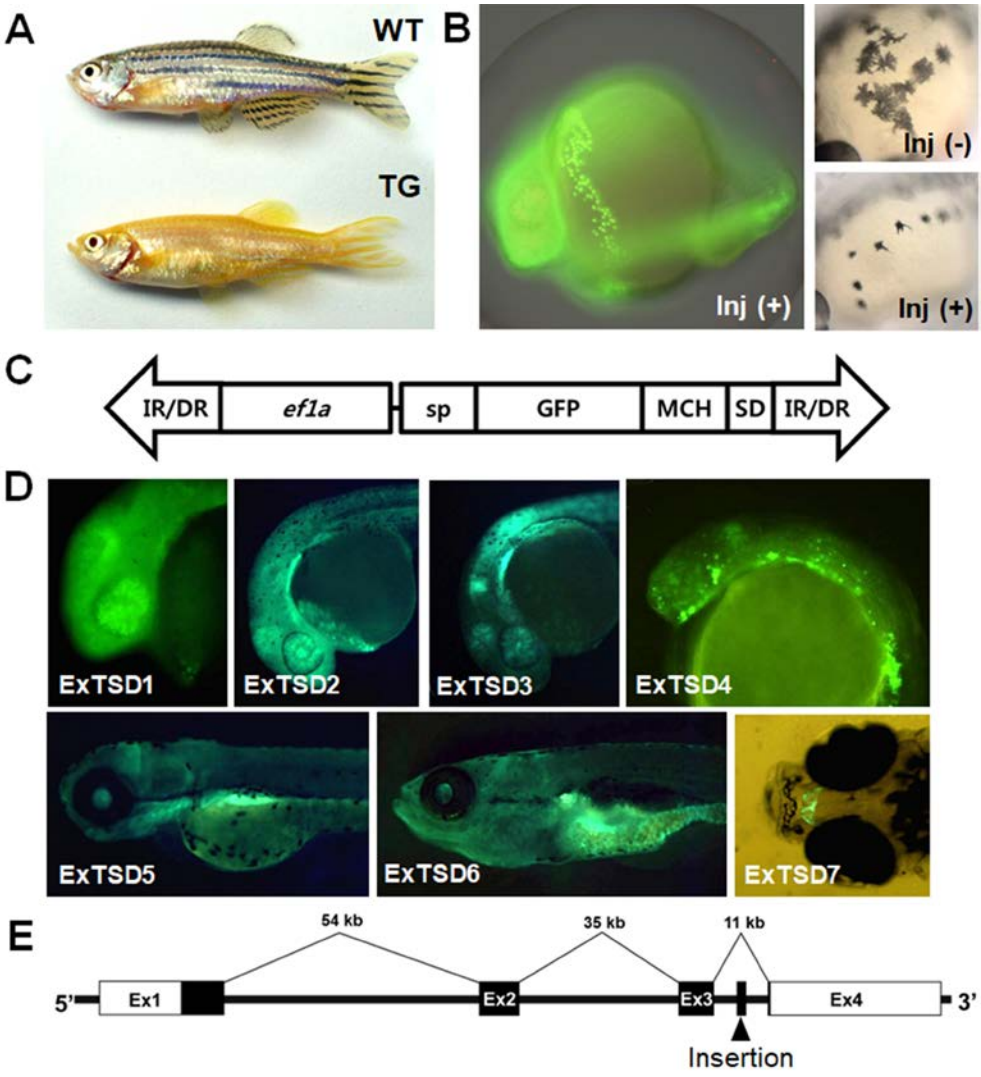

Figure S1. Dual reporter system used for insertional mutagenesis, the golden fish project. (**A**) Body color change in MCH-expressing transgenic zebrafish (TG, a *cmv:mch tg* line), compared to wild-type adult fish (WT). (**B**) Expression of dual reporter, GFP-MCH fusion protein, in *ef1a:gfp-mch*-injected zebrafish embryos. GFP fluorescence and melanosome aggregation are detectable in injected embryos, inj (+), compared to un-injected control embryo, inj (-). (**C**) Structure of a gene trap vector used in insertional mutagenesis. IR/DR; inverted repeat/direct repeat element; *ef1a*, *elongation factor 1 alpha* (*ef1a*) gene promoter; sp, signal peptide; GFP; green fluorescent protein; MCH, melanin-concentrating hormone; SD, splice donor. (**D**) Representative mutants showing GFP expression in various tissues (ExTSD1-7; images not to scale). (**E**) Mapping of the insertion site (arrow) in the intron 3 of a *samdori* gene on chromosome 4.

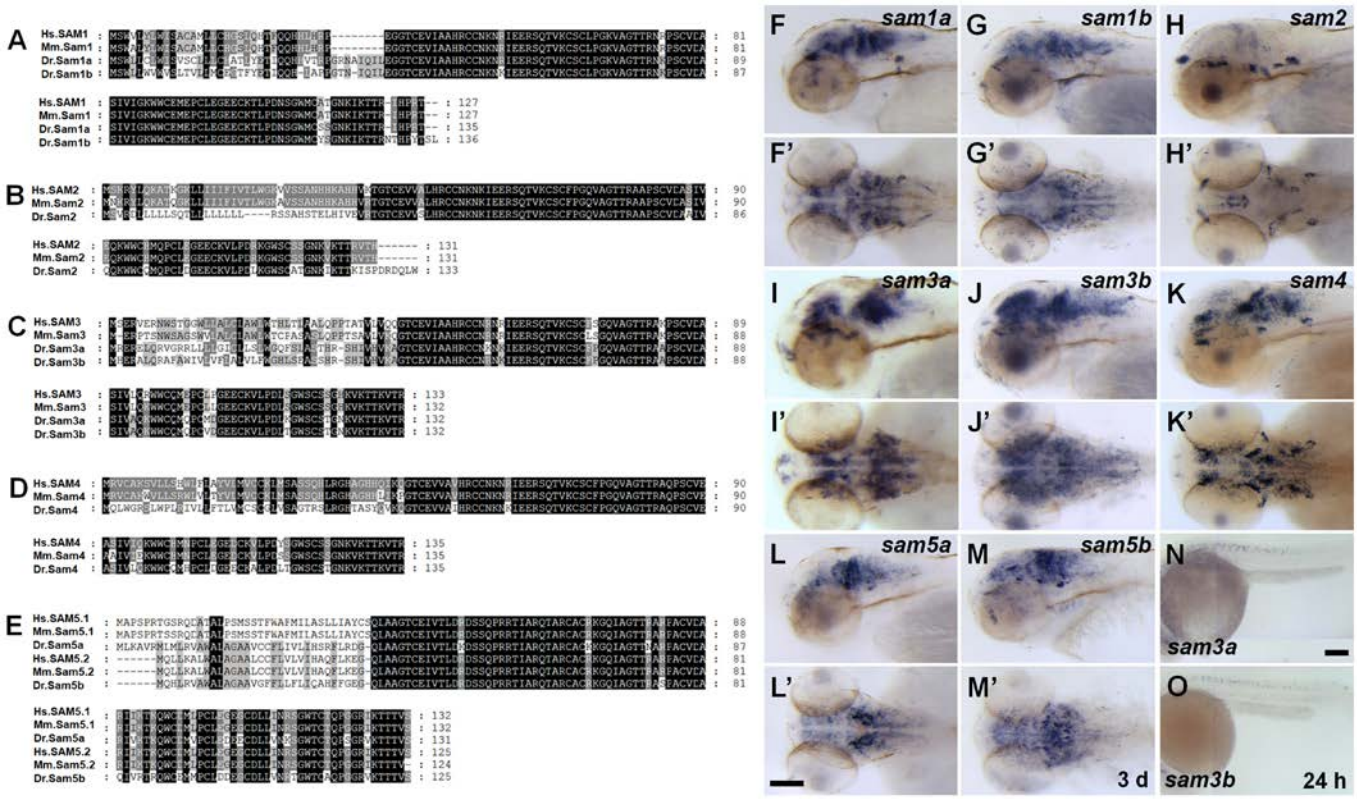

Figure. S2. Conserved synteny and CNS-specific expression of *samdori* gene family. (**A**) Alignments of zebrafish sam1a and sam1b amino acids with that of human SAM1 and mouse Sam1 (Genbank accession for human and mouse, NM_213609; NM_182808, respectively). (**B**) Alignments of zebrafish sam2 amino acids with human SAM2 and mouse Sam2 (NM_178539; NM_182807). (**C**) Alignments of zebrafish sam3a and sam3b amino acids with human SAM3 and mouse Sam3 (NM_182759; NM_183224). (**D**) Alignments of zebrafish sam4 amino acid with human SAM4 and mouse Sam4 (NM_001005527; NM_177233). (**E**) Alignments of zebrafish sam5a and sam5b amino acids with human SAM5.1, SAM5.2 and mouse Sam5.1, Sam5.2 (NM_001082967; *NM_015381; NM_001252310; NM*_134096). **(F-O)** Whole-mount *in situ* hybridization was performed to detect the expression of mRNAs. All *sam* gene family members are exclusively expressed in the brain. Three day-old (3d) embryos (**F-M'**). *sam3a and sam3b show*ed additional expression in the spinal cord at 24 h, lateral views (**N**, **O**). Lateral views (**F-M**). Dorsal views (**F'-M'**). Scale bar, 100 µm.

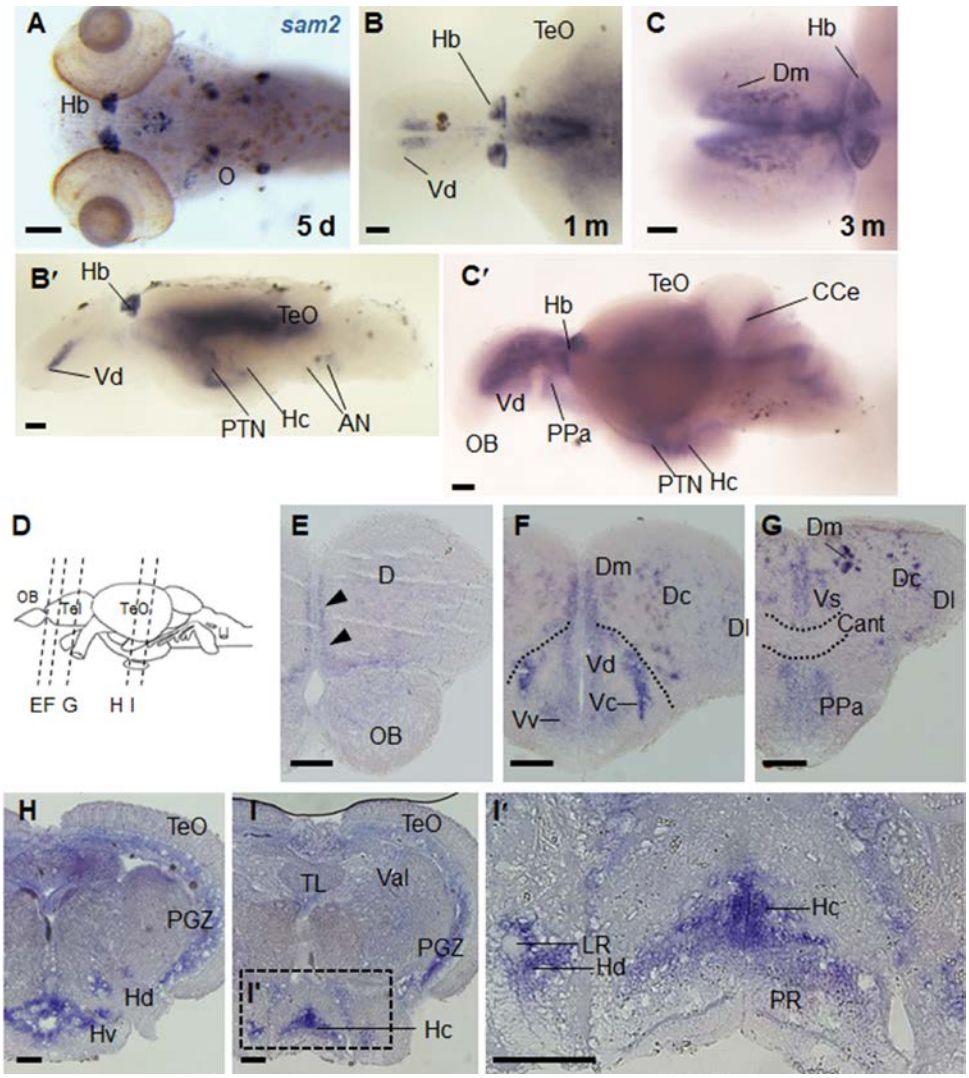

Figure. S3. Expression of *sam2* in the larval and adult brain. Whole-mount *in situ* hybridization of *sam2* in larva and adult (1- and 3-month; 1 m, 3 m) **(A)** *sam2*-expressing cells in 5 day-old larvae. Habenula (Hb) expression is already prominent at this stage. Expression in the otic neurons (O) is also seen. **(B, B')** At 1-month, expression of *sam2* in the brain. Dorsal telencephalic view **(B)** and lateral view **(B')**. **(C, C')** *sam2* expression in the adult brain. Dorsal telencephalic view **(C)** and lateral view **(C')**. **(E-I')** Serial sections of adult brain. Levels of the cross-sections are indicated in **(D)**. Scale bar, 100 µm. AN, auditory nerve; Cant, anterior commissure; CCe, corpus cerebelli; D, area dorsalis telencephlali; Dc, central zone of area dorsalis telencephali; Dl, lateral zone of area dorsalis telencephali; Dm, medial zone of area dorsalis telencephali; Hc, caudal zone of periventricular hypothalamus; Hd, dorsal zone of periventricular hypothalamus; Hv, ventral zone of periventricular hypothalamus; LR, lateral recess of diencephalic ventricle; OB, olfactory bulb; PGZ, periventricular gray zone; PPa, parvocelluar preoptic nucleus, anterior part; PR, posterior recess; PTN, posterior tuberal nucleus; TeO, optic tectum; TL, torus longitudinalis; Val, lateral division of vlvula cerebelli; Vc, central nucleus of area ventral telencephali; Vd, dorsal nucleus of area ventral telencephali; Vs, supracommissural nucleus of area ventral telencephali; Vv, ventral nucleus of area ventral telencephali.

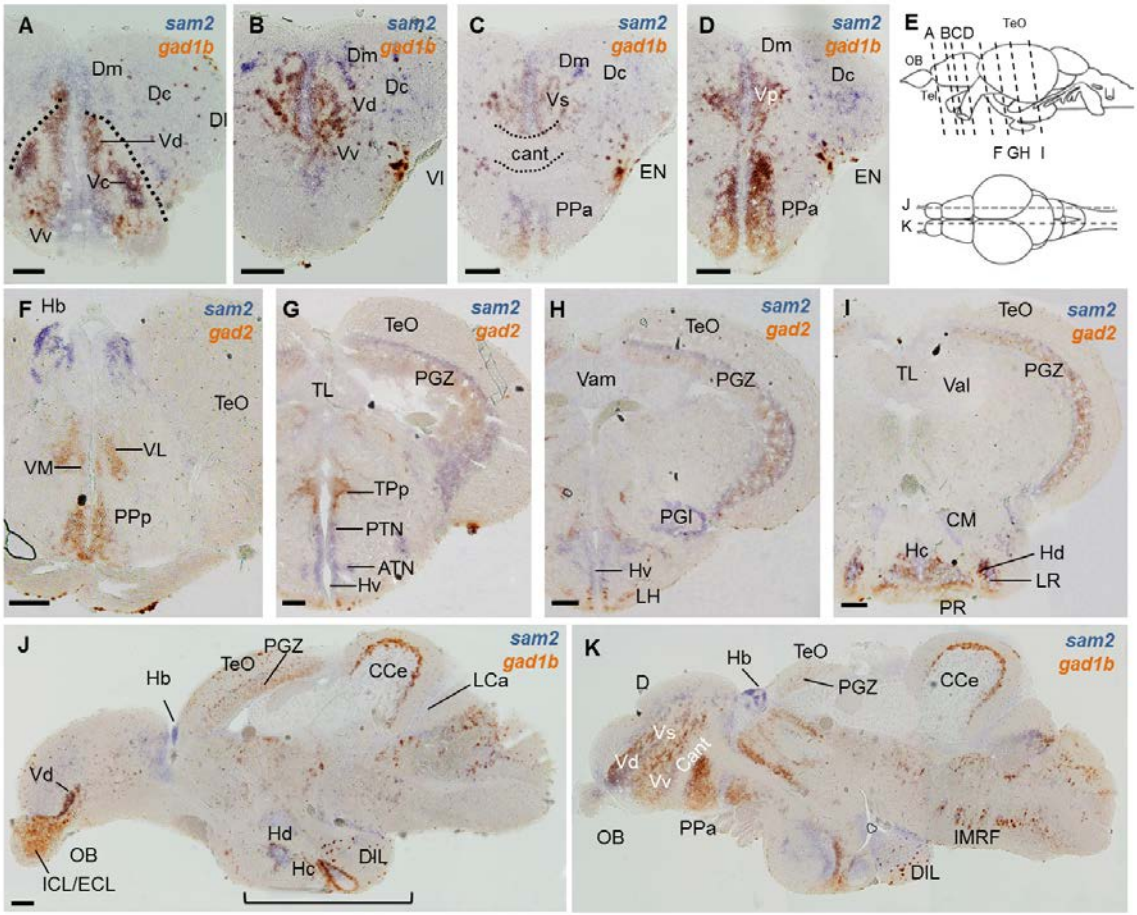

Figure. S4. Two color *in situ* hybridization of *sam2* with *gad1b* or *gad2* in adult brain. (A-D) Cross section of telencehpalic region. **(F-I)** Cross section of diencephalic area. **(J, K)** Sagittal section of whole brain. Expression region of *sam2* is partially overlapped by that of *gad1b* in several brain regions, including telencephalon and hypothalamus. Levels of the sections (top, cross section; bottom, sagittal section) are indicated in **(E)**. Scale bar, 100 μm. ATN, anterior tuberal nucleus; Cant, anterior commissure; CCe, corpus cerebelli; CM, corpus mamillare; D, area dorsalis telencephlali; Dc, central zone of area dorsalis telencephali; DIL, diffuse nucleus of the inferior lobe; Dl, lateral zone of area dorsalis telencephali; Dm, medial zone of area dorsalis telencephali; ECL, external cellular layer of olfactory bulb; EN, entopedunclular nucleus; Hc, caudal zone of periventricular hypothalamus; Hd, dorsal zone of periventricular hypothalamus; Hv, ventral zone of periventricular hypothalamus; ICL, internal cellular layer of olfactory bulb; IMRF, intermediate reticular formation; LCa, caudal lobe of the cerebellum; LH, lateral hypothalamic nucleus; LR, lateral recess of diencephalic ventricle; OB, olfactory bulb; PGl, lateral preglomerular nucleus; PGZ, periventricular gray zone; PPa, parvocelluar preoptic nucleus, anterior part; PPp, parvocellular preoptic nucleus, posterior part; PR, posterior recess; PTN, posterior tuberal nucleus; TL, torus longitudinalis; TPp, periventricular nucleus of posterior tuberculum; Val, lateral division of vlvula cerebelli; Vam, medial division of valvula cerebelli; Vc, central nucleus of area ventral telencephali; Vd, dorsal nucleus of area ventral telencephali; VL, ventrolateral thalamic nucleus; VM, ventromedial thalamic nucleus; Vp, Ventral pallium; Vs, supracommissural nucleus of area ventral telencephali; Vv, ventral nucleus of area ventral telencephali.

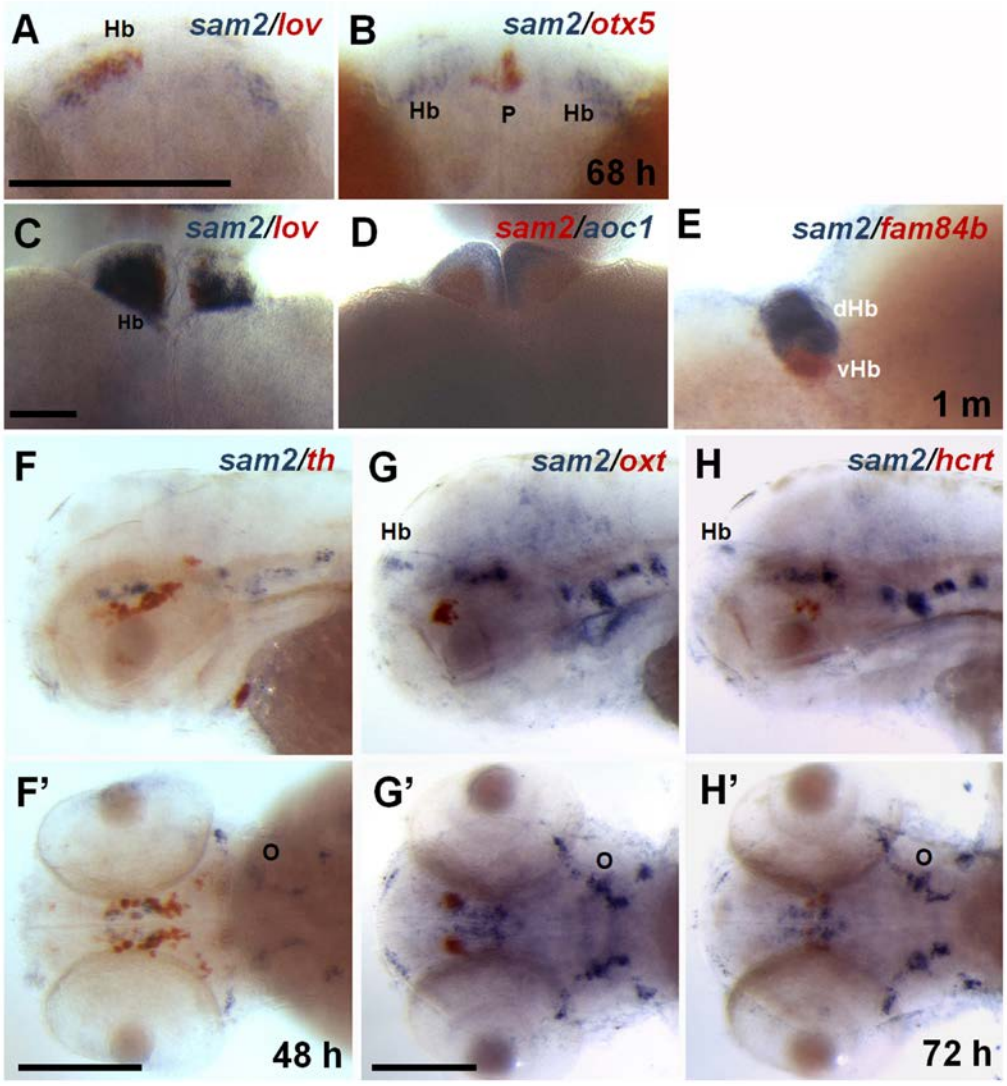

Figure. S5. Characterization of *sam2*-expressing cell populations in larval zebrafish. Two-color whole-mount *in situ* hybridization was performed to identify *sam2*-positive cells, comparing with known habenula (Hb) markers: *lov* (*kctd12.1*), dorsal Hb (dHb); *aoc1*, ventral Hb (vHb); *fam84b*, both dHb and vHb marker; *otx5*, pineal organ (p) marker. (**A**, **B**) 68 hour-old larvae. Dorsal view. (**C**-**E**) Adult brain. Dorsal view, except for lateral view in (**E**). Note the specific expression of *sam2* in the dorsal Hb. Other than Hb, *sam2*-expressing cells do not overlap with markers of dopaminergic neurons (*th at 48h*; **F**, **F'**), oxytocinergic neurons (*oxt* at 72h; **G**, **G'**), and hypocretinergic neurons (*hcrt* at 72h; **H**, **H'**). **F**-**H**, lateral view; **F'**-**H'**, dorsal view. Scale bar, 200 µm.

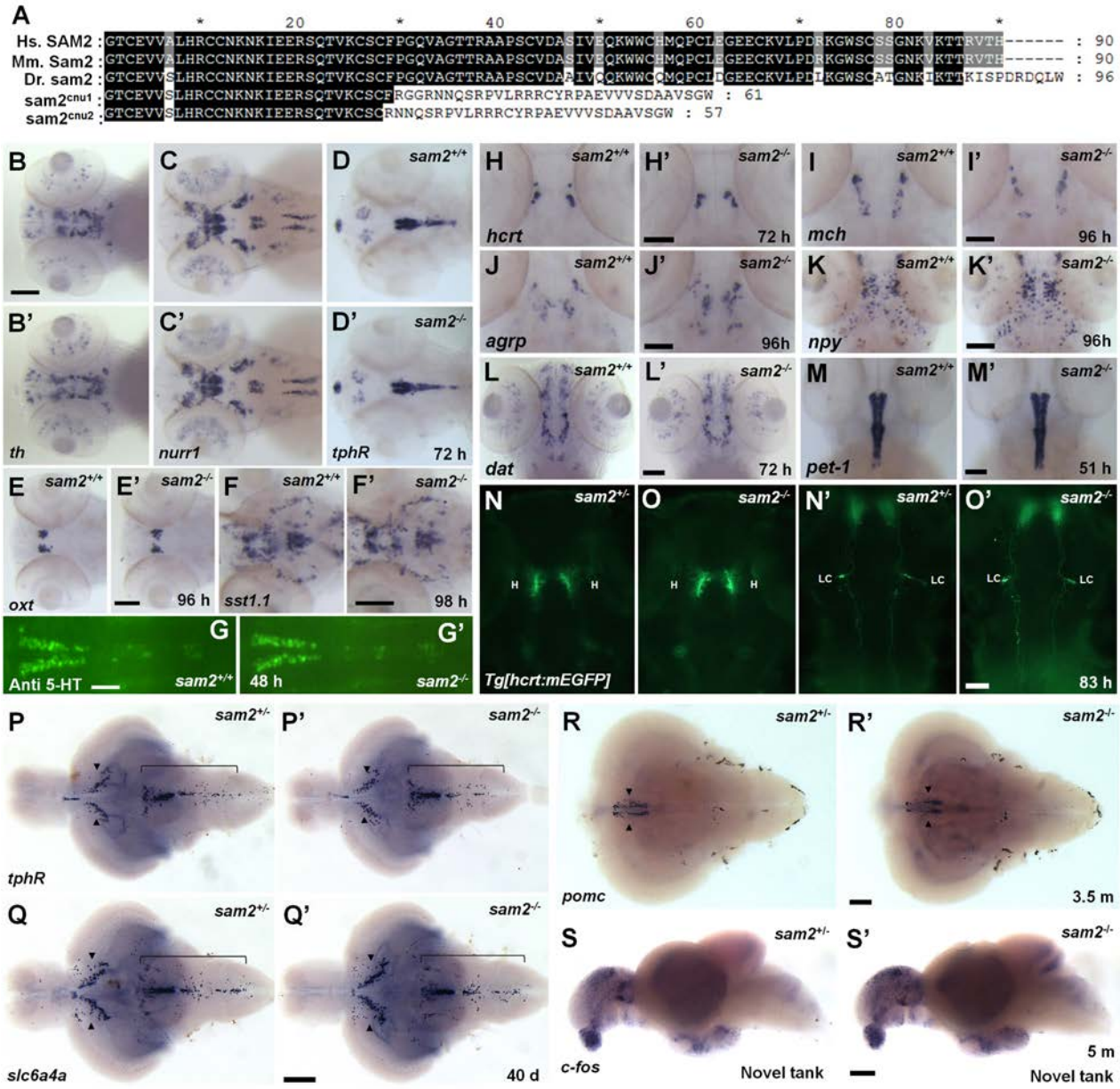

Figure. S6. Normal expressions of various neuronal markers in *sam2*^{cnu1} KO fish. (**A**) Alignment of human, mouse, and zebrafish Sam2 peptides. Putative amino acid sequences of mutant forms are also aligned. Dopaminergic neuron (*th*, **B-B'**; *nurr1*, **C-C'**; *dat*, **L-L'**), serotonergic neuron (*tphR*, **D-D'**; 5-HT, **G-G'**; *pet-1*, **M-M'**), oxytocinergic neuron (*oxt*, **E-E'**), and IPN (*sst1*, **F-F'**) markers. Additional neural markers: *hcrt* (**H-H'**), *mch* (**I-I'**), *agrp* (**J-J'**), and *npy* (**K-K'**). (**N-O'**) Normal hypothalamus (H) - locus coeruleus (LC) axonal connections in *sam2*^{cnu1} KO fish as judged by *Tg[hcrt:EGFP]* transgene expression. Dorsal views, anterior to the top. Scale bar, 100 μm. (**P-R'**) Serotonergic neuron (*tphR*, *slc6a4a*) and adrenocorticotropic hormone precursor *pomc* marker in adult brain. Arrowheads indicate the ventral posterior tuberculum (**P-Q'**) and the nucleus lateralis tuberis (**R**, **R'**). Bracket defines the raphe (**P-Q'**). (**S-S'**) *c-fos* expression in the novel tank assay. Scale bar, 500 μm.

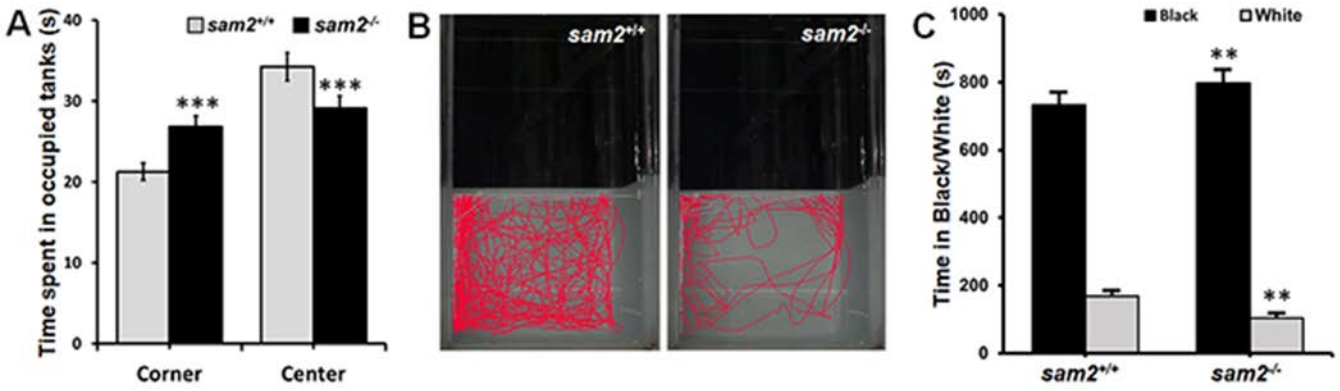

Figure. S7. *sam2*^{cnu1} KO fish show anxiety behavior in open tank and scototaxis tests. (**A**) In the open tank, thigmotaxis was measured by comparing the mean time spent in the tank's corner (one fifth of tank's left and right part) vs. its center (rest of corner of the tank) every 1 min interval for 30 min (*sam2*$^{+/+}$, n = 12; *sam2*$^{-/-}$, n = 12; Corner, Cohen's d = 0.93, Mann-Whitney U = 908, P = 0.00001; Center, Cohen's d = 0.81, Mann-Whitney U = 982, P = 0.00001). (**B**) Scototaxis test. Movement tracking of control and *sam2* KO fish in the black/white tank. Red lines indicate the locomotion of fishes recorded only in the white arena. (**C**) Total time in black or white arena (second, s) (*sam2*$^{+/+}$, n = 18; *sam2*$^{-/-}$, n = 24; Black arena, Cohen's d = 1.07, Mann-Whitney U = 96, P = 0.0083, White arena, Cohen's d = 0.76, Mann-Whitney U = 95.5, P = 0.008).

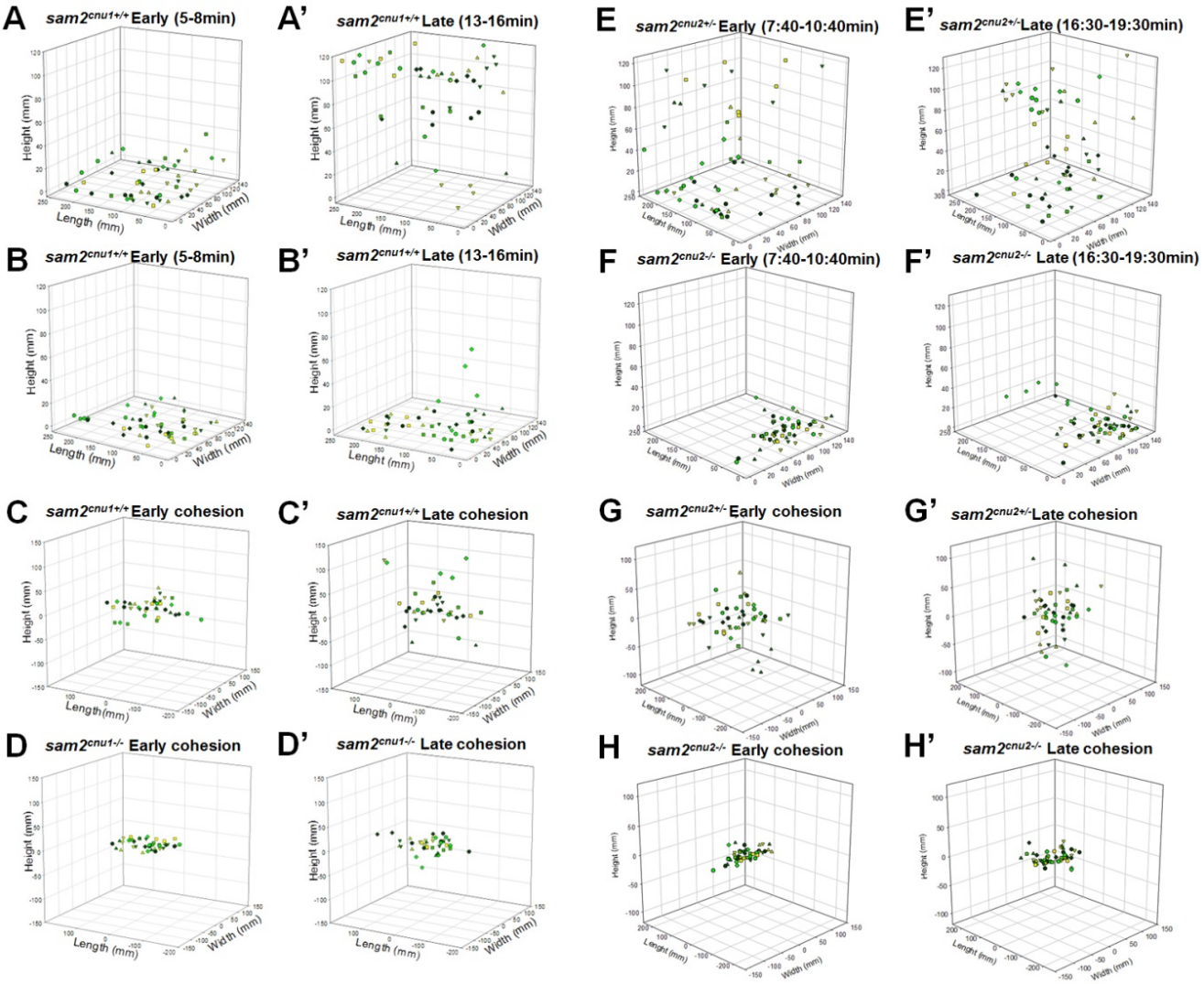

Figure. S8. Increased anxiety (A-B' and E-F') and social cohesion (C-D' and G-H') in two different *sam2* KO fish lines (*sam2*^{cnu1} and *sam2*^{cnu2}). Three-dimensional reconstructions of video trackings before habituation (early) and after habituation (late) to the new environment. Five or six fish were placed as a group in a novel tank. Different color spots indicate the actual position of individual fish in 20-second intervals of video recording (10 points for each fish). (**C-D'**, **G-H'**) Increased social cohesion in *sam2* KO fish. The focal fish is positioned in the center of the space and the relative position of its shoal members are indicated by different color spots. We measured the distance between the focal fish and one of its shoal members before habituation (early) and after habituation (late) to the new environment (*sam2*$^{cnu1+/+}$and *sam2*$^{cnu1-/-}$, n = 5; *sam2*$^{cnu2+/+}$ and *sam2*$^{cnu2-/-}$, n = 6).

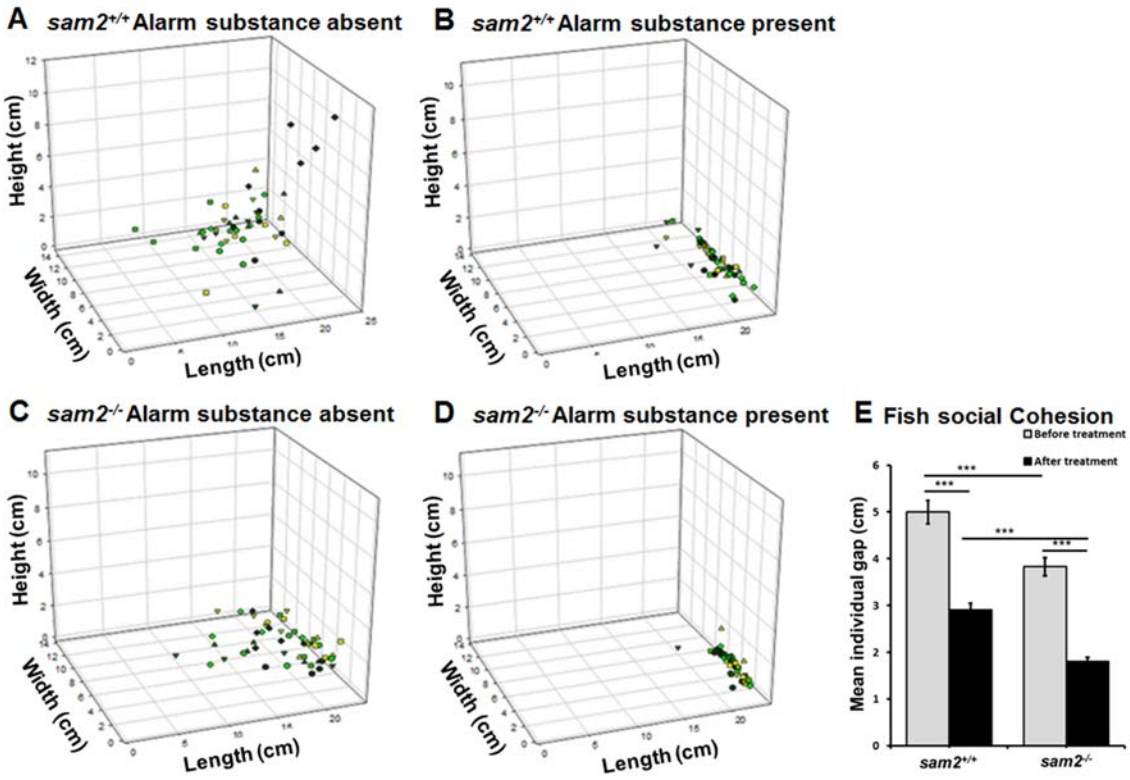

Figure. S9. Increased social cohesion of *sam2*^{cnu1} KO fish under fear-inducing condition. Five adult male fish were kept in a novel tank for 30 min and then treated with alarm substance. (**A**-**D**) Temporal three-dimensional reconstructions of video tracking before and 15 min after treatment of alarm substance. Different color spots indicate the actual positions of individual fish determined at 20-second intervals during 3-min-video recording (10 points for each fish). (**E**) Measurement of soc ial cohesion as the mean individual gap. ***P < 0.001; Student's t-test.

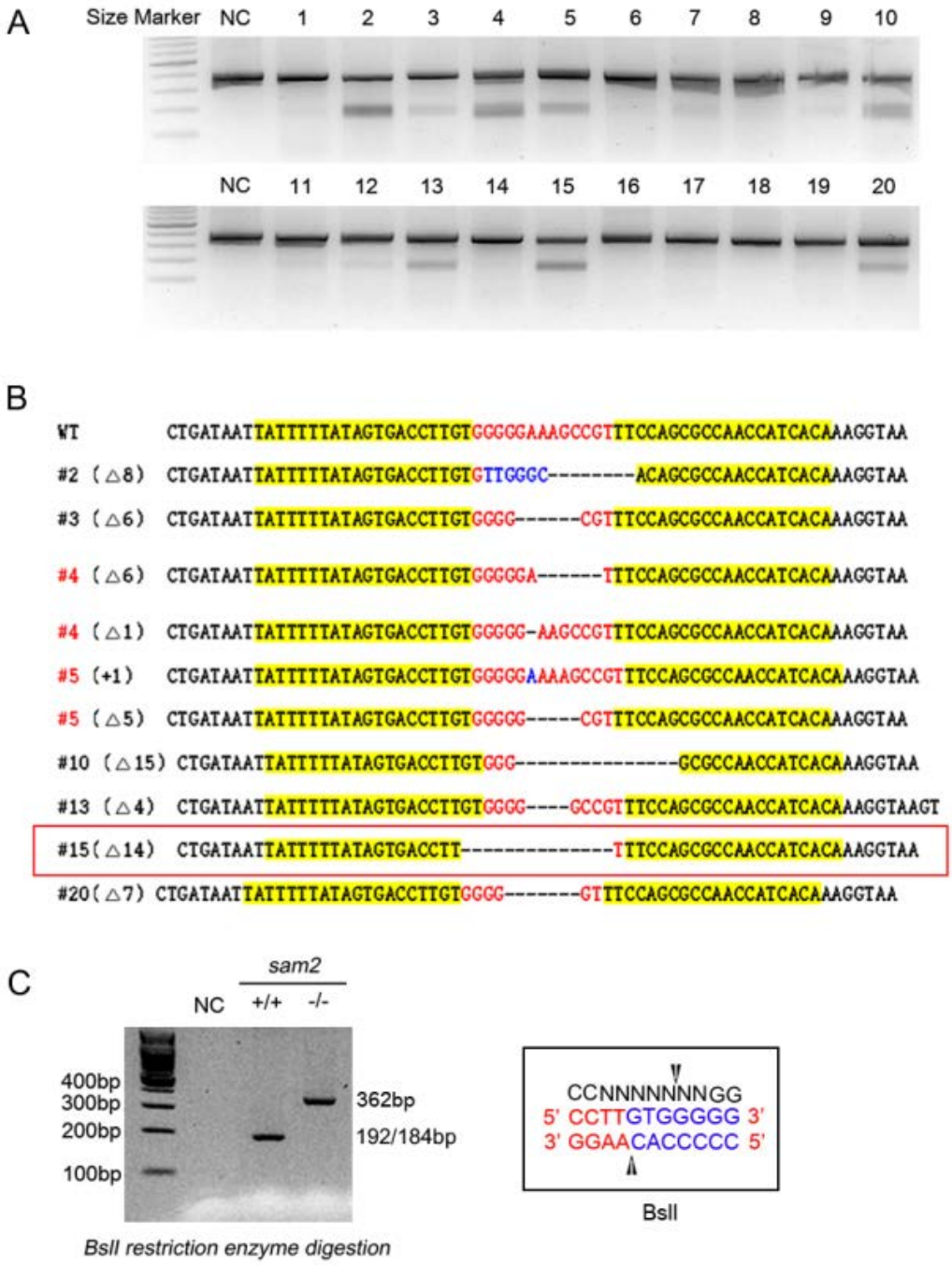

Figure. S10. Generation of TALEN-mediated *Sam2* KO mice (**A**) Founders of *Sam2* KO mice were identified with T7E1 assay. (**B**) Sequence alignments of various *Sam2* KO alleles. Selected *Sam2* mutant allele marked by a red box contains a 14 bp-deletion which causes a frameshift leading to a premature stop codon. (**C**) Genotyping results with PCR and *BslI* restriction enzyme digestion. Due to the 14 bp-deletion, mutant allele was not digested with *BslI*. Wild (*Sam2*$^{+/+}$): 184 and 192 bp; Knockout (*Sam2*$^{-/-}$): 362 bp. *BslI* enzyme digestion sequence is shown in the box. Sequence in blue was deleted in *Sam2* mutant allele.

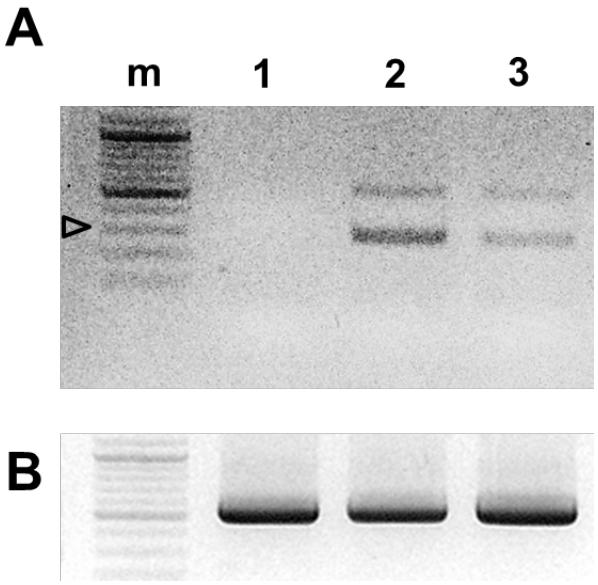

Figure. S11. RT-PCR analysis of *Sam2* expression in the mouse brain. (**A**) For reverse transcription-polymerase chain reaction (RT-PCR) analysis, total RNA was isolated from the dissected tissues after cryosection of frozen mouse brain. *Sam2* was highly expressed in the hippocampus and habenula but was hardly detected in the paraventricular nucleus (PVN). m, size markers; 1, PVN; 2, hippocampus; 3, habenula. Arrow head indicates 300 bp size marker. (**B**) *Beta-actin* (*Actb*) was used as an endogenous control.

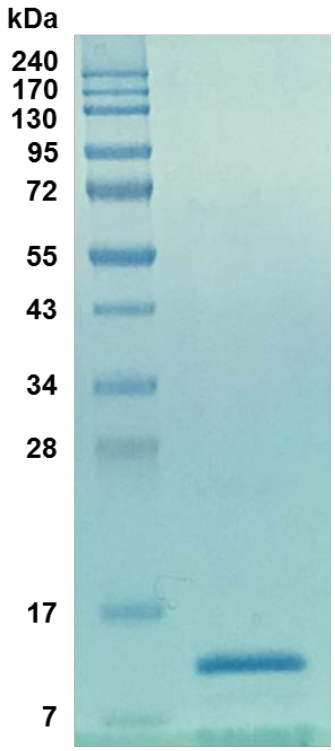

Figure. S12. SDS-PAGE gel analysis of purified SAM2 protein. For high purity protein production, the eluted protein after on-column cleavage was further purified on HiTrap Q HP column. The purity and molecular weight (~12 kDa) of SAM2 protein was confirmed by 10% SDS-PAGE analysis, using the protein size marker.

Supplementary Table 1. Summary of expression pattern of *sam2* in the adult zebrafish.

	sam2	Homologous region in tetrapod telencephalon
Dm	++	pallial amygdala
Dc	scattered	cortex
Dl	-	hippocampus
Dp	-	not applicable
Vd	++	striatum
Vc	++	not applicable
Vv	++	striatum and/or strially-derived septum
Vs	+	ventral part of central amygdala
PTN	+	ventral tegmental area
PPa	+	paraventricular nucleus (PVN)
PPp	+	paraventricular nucleus (PVN)
Hb	++(dorsal)	medial habenula
PGZ	+	
Hc	++	hypothalamus
Hd	++	hypothalamus
Hv	++	hypothalamus
CCe	+	
LCa	-	
EG	-	

Abbreviations: Dm, medial zone of area dorsalis telencephali; Dc, central zone of area dorsalis telencephali; Dl, lateral zone of area dorsalis telencephali; Dp, posterior zone of are dorsalis telencephali; Vd, dorsal nucleus of area ventral telencephali; Vc, central nucleus of area ventral telencephali; Vv, ventral nucleus of area ventral telencephali; Vs, supracommissural nucleus of area ventral telencephali; PTN, posterior tuberal nucleus; PPa, parvocelluar preoptic nucleus, anterior part; PPp, parvocellular preoptic nucleus, posterior part; Hb, Habenula; PGZ, periventricular gray zone; Hc, caudal zone of periventricular hypothalamus; Hd, dorsal zone of periventricular hypothalamus; Hv, ventral zone of periventricular hypothalamus; CCe, corpus cerebelli; LCa, caudal lobe of the cerebellum; EG, eminentia granularis.